MORPHOLOGICAL VARIATION IN THE HUMAN TIBIA AND ITS POTENTIAL FOR PROFILE ESTIMATION IN HUMAN SKELETAL REMAINS

A Thesis By

Christle Shannon Arney

B.A., University of Tennessee, Knoxville, 2006

Submitted to the Department of Anthropology
and the faculty of the Graduate School of
Wichita State University
in partial fulfillment of
the requirements for the degree of
Masters of Arts

December 2011

MORPHOLOGICAL VARIATION IN THE HUMAN TIBIA AND ITS POTENTIAL FOR PROFILE ESTIMATION IN HUMAN SKELETAL REMAINS

The following faculty members have examined the final copy of this thesis for form and content, and recommend that it be accepted in partial fulfillment of the requirement for the degree of Masters of Arts with a major in Anthropology.

_____

Peer H. Moore-Jansen, Committee Chair

_____

Robert Lawless, Committee Member

_____

Leland Russell, Committee Member

DEDICATION

To my parents,

my Taylor Bug,

and Nana

Thank you for always believing in me, and

for supporting and loving me through it all.

The only true guardian of peace lies within:
a sense of concern and responsibility for your own future and
an altruistic concern for the well-being of others.

~The Dalai Lama

ACKNOWLEDGEMENTS

I would like to acknowledge and express my extreme gratitude to those individuals whose encouragement and assistance aided in the completion of this thesis.

I would first like to thank Dr. Peer H. Moore-Jansen who served as my advisor and mentor over the course of my Masters degree, as well as the committee chair of my thesis committee. Your abundant knowledge, insight and motivation have contributed to the success of my Master's thesis, as well as the overall success of my graduate career. This experience has not only served to enhance my knowledge and practical exposure to biological anthropology, but has also served to heighten my passion for human skeletal biology and ensured my continuation on this career path. Thank you for your guidance and support over these years; your contributions will forever guide me as an anthropologist.

I would also like to thank Dr. Robert Lawless and Dr. Leland Russell for putting forth their time and effort to serve as members of my thesis committee. Your insight and feedback has proved invaluable.

I express my tremendous appreciation to the Nancy J. Berner Fund for its financial contribution which enabled my research at the Hamman-Todd Osteological Collection. This support provided through the Anthropology Department at Wichita State University made the research expenses less burdensome, allowing me to travel to the Cleveland Museum of Natural History in Cleveland, Ohio, in order to collect the data associated with this study. Further, I would like to thank the faculty and curator of the Hamman-Todd Osteological Collection for providing me access to the collection. I am specifically grateful to Lymann Jellema for your knowledge and assistance which aided in the timely completion of the data collection process.

I have been privileged with a great support network at Wichita State University whose friendship, guidance and motivation have been an essential part of my graduate experience. I am appreciative to the numerous individuals that assisted with the testing of the reliability of my measurement protocol which greatly contributed to the success of this thesis. I would especially like to thank Ivy Davis, Joana Soltis and Meghan Voisin for their constant support and reassurance inside and outside the classroom. You have truly made this experience an unforgettable one, and I look forward to creating many more throughout the years.

I would like to thank my remarkable parents who allow me to chase my dreams, no matter where they take me. I would not be who I am today if it wasn't for your profound love, support and encouragement. Thank you for never limiting me as a person or in my academic and career aspirations. I would also like to thank my Nana for always believing in me. The memories we have created will forever be a part of me and are partially responsible for making me into the person I have become. Finally, I would like to extend my love and thanks to my beautiful sister, Taylor. You have been and continue to be my strength. You give me meaning.

ABSTRACT

This study evaluates the existence and degree of human variation as it is represented by the morphology of the tibia. Specifically, this research is undertaken in order to quantitatively address the morphological variation of this skeletal element to reveal the inherent variation within the individual, while also evaluating the discrepancies that result due to the sex and age of an individual. It also explores the interaction of tibial morphology with living stature, assessing the ability of the quantified portions of the bone to explain stature. In order to investigate this variation, the tibiae of 382 mature skeletal remains from the Hamann-Todd Osteological Collection in Cleveland, Ohio, were analyzed. These specimens were comprised of 180 females and 202 males whose group affiliation were designated as American Black.

Using univariate and multivariate analyses, the morphological variation of the human tibia was assessed in respect to goals outlined above. These analyses revealed the manner by which dimensions of the tibia covaries, providing a better understanding of the innate variation that exists within this bone. These procedures also enabled the evaluation of sex and age effects on the size and shape of the tibia, revealing that the variations due to sex are profound enough to allow accurate classification of the sexes from the morphology of the tibia. While age related changes impact the morphology of the bone, they do not impede the ability of the dimensions to be used as reliable sex indicators. Further, the assessment of the interaction of the tibia and stature demonstrates the degree by which the variables explain the stature variation in the sample, attesting to the capacity of the tibial dimensions to be used as predictors of stature. Finally, the efficacy of particular measurements employed throughout this study to obtain accurate information concerning human variation is established, as well as their applicability to fragmentary remains.

TABLE OF CONTENTS

TABLE OF CONTENTS (continued)

LIST OF TABLES

LIST OF TABLES (continued)

LIST OF TABLES (continued)

LIST OF FIGURES

Figure Page

CHAPTER ONE

INTRODUCTION

Skeletal remains offer an incredible source of information concerning the study of human variation, both temporally and spatially. This area of research not only contributes to an improved understanding of the natural aging processes the human skeleton endures, but also provides insight into the impact of differing cultural, environmental and biological factors on human lifeways and behavior as it is represented by human skeletal remains. Understanding variation as it is expressed at the individual and population level, as well as over time and space is essential to the biological reconstruction of past populations and the identification of unknown human remains. The study of human variation is typically employed to discern and comprehend the nature of this variation in respect to age, sex and group affiliation, as well as the interaction of these variables.

Statement of Purpose

This study is multifaceted, aiming to evaluate human morphological variation as it is represented by tibial dimensions, while also analyzing the effect of sex and age on this variation. Through these endeavors this research quantitatively assesses the size and shape variation of the tibia inherent in the individual, as well as the degree to which age and sex may aid in the explanation of tibial morphology. Further, the measurements affiliated with this study were selected to illustrate how indicative the morphology of the tibia is concerning the sex of an individual. This research also investigates how tibial variability interacts with stature in an effort to utilize this variation to accurately reconstruct living stature. Pivotal to this study are the

hypotheses that the tibial dimensions will represent the size and shape variation expressed between males and females and differing age groups, as well as how they vary in reference to stature.

This study has multiple implications concerning the field of anthropology, specifically biological and archaeological anthropology. Not only is this study essential to the overall understanding of human variability, but it also provides insight into the predictability of sex and stature from skeletal remains. This aids in the identification of modern human remains, as well as demographic reconstruction in archaeological and paleoanthropological settings. In addition, the assessment of stature may allude to the subsistence patterns, health, nutrition, and disease of past and present human populations, while also enabling research into human adaptations and secular change.

The following chapters detail the background, materials and methods, results and discussion associated with this research. The second chapter consists of the background information relevant to the study presented here. This includes an overview of the musculoskeletal system associated with the tibia, as well as the growth and development and degenerative processes that affect the bone. This section also details sexual dimorphism and secular variation as it impacts the human skeleton and living stature. Finally, this chapter incorporates a conspectus of relevant research concerning the tibia and stature reconstruction. The third chapter is comprised of the materials and methods which outline the sampling, measurement, and statistical protocols utilized in this study. It also recounts the history of the collection from which the sample was derived. The fourth chapter reports the results of the

associated univariate and multivariate statistical analyses implemented during this research, while the final chapter discusses these results in respect to the study at hand.

CHAPTER TWO

BACKGROUND

Introduction

This study addresses the morphological variation inherent among *Homo sapiens* as it is represented by the tibia. In particular, the relationship between morphometric variation and sex, age, and living stature is evaluated. In order to fully comprehend these relationships, it is necessary to review the anatomy of the tibia and the developmental and degenerative processes that affect this long bone. This chapter also discusses the variation that exits with the above processes, as well as the affects of sexual dimorphism and secular variation on both skeletal morphology and stature in an effort to account for any variation or innate biases that may be represented by the sample in this study. Finally, the chapter recounts relevant research concerning the affiliation of stature and skeletal elements.

The Tibia: An Anatomical Overview

The tibia, commonly referred to as the shin bone, is one of three long bones comprising the lower extremity (Figure 1). The femur and those structures of the proximal portion of the lower extremity are referred to as the thigh, while the tibia, fibula and related structures are the leg. The term long bone is used in reference to those bones of the postcranial skeleton that are "longer than they are wide" and possess both a diaphysis (shaft) and an epiphysis (end plate) (Schwartz, 1995). Articulation occurs between the tibia and three bones: the femur proximally, the talus distally, and the fibula both proximally and distally along the postero-lateral surface (Scheuer and Black, 2000). The tibia is a bilateral structure that forms the medial portion of the

leg (Figure 2). It is largest at the proximal end and becomes progressively smaller as the shaft descends, taking on a "prismoid" shape (Gray, 2010). The distal end is slightly widened in comparison to the shaft. As a load bearing bone, the tibia is responsible for supporting the weight of the skeleton, as well as aiding in locomotion (Carter, 2000). Mobilization of the leg is enabled through the major joints and muscles associated with the tibia. Its location in the lower leg allows it to further assist in the distribution of weight between the femur and the talus (Steele & Bramblett, 1988).

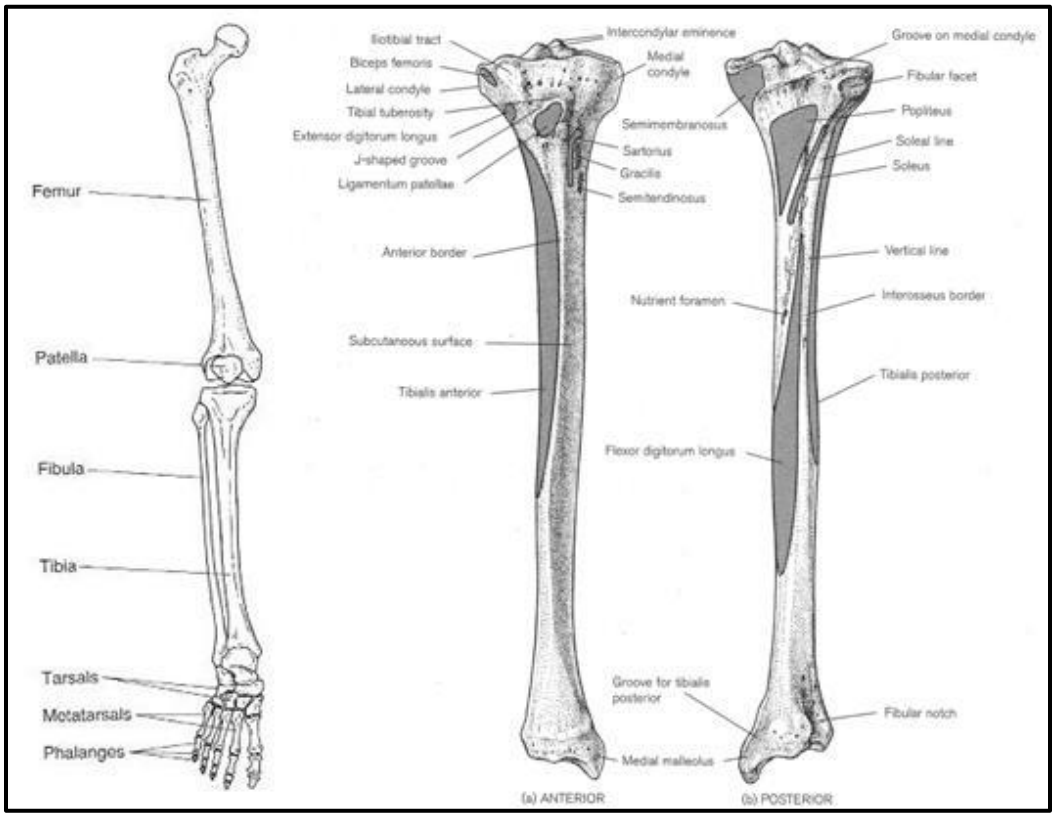

Figure 1-2. *The right lower extremity. (Fig. 1, left) After Scheuer and Black 2004:34, Right adult tibia. (Fig. 2, right) After Scheuer and Black 2000:*400.

The Proximal End

Due to its position and function in the human body, the proximal end of the tibia is comprised of multiple distinguishing features (Figure 3). The tibial plateau is located at the proximal surface of the tibia and is the broadest portion of the bone. It consists of two articulating surfaces, the medial and lateral condyles, both of which articulate with the distal end of the femur, creating the hinge joint of the knee.

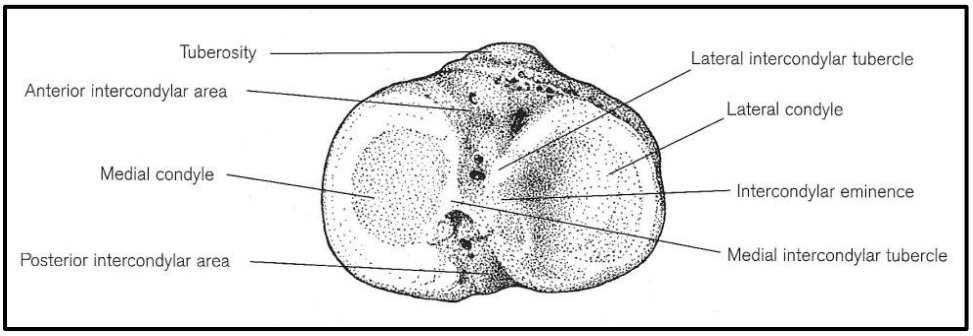

Figure 3. *Proximal articular surface of right adult tibia. After Scheuer and Black 2000:401.*

Each condyle displays similarities, and are characterized by a convex center and a flattened periphery, taking on the reciprocal shape of the femur's medial and lateral condyles, which are further adapted to one another due to articular discs, or menisci, that separate the two bones (Carter, 2000). However, the condyles are discernible from one another due to their unique shapes. The medial condyle is ovoid, "with its long axis running antero-posteriorly," while the lateral condyle is slightly smaller and "more circular in shape" (Scheuer & Black, 2000). Separating these condyles from one another is the intercondylar eminence. This is a raised area of the proximal surface distinguished by medial and lateral projections that commonly form a valley at the center of the intercondylar eminence. Located approximately two centimeters

below the anterior margin of the tibial plateau is the tibial tuberosity. This is a roughened prominence that serves as the attachment site for the ligamentum patellae, and typically varies in size between individuals (Scheuer & Black, 2000).

The Diaphysis

The size and shape of the shaft varies greatly between individuals, but its cross-section maintains a regular, triangular form (Figure 4). The shaft is broadest proximally and gradually narrows progressing toward the distal end. This narrowing terminates at the lower fourth of the bone which is also the location of most tibial fractures. It is here that the enlargement of the shaft initiates once again.

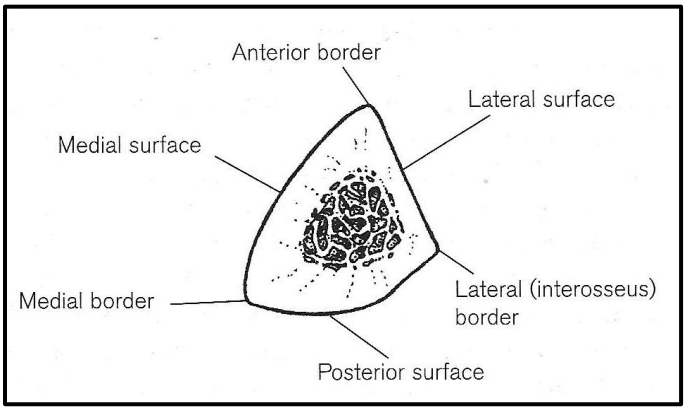

Figure 4. *Cross-section of adult tibia in middle third of shaft. After Scheuer and Black 2000:402.*

The shaft is described as having "three borders and three surfaces" (Gray, 2010). The anterior border creates a prominent ridge that descends from the iliotibial tract down to the anterior portion of the medial malleolus, a projection on the medial side of the distal end that forms the medial aspect of the ankle. The lateral border, also known as the interosseous crest,

extends from the anterior side of the articulating surfaces with the fibula, known as the fibular facet proximally and the fibular notch distally. This border maintains itself as a sharp crest for the majority of its length and serves as the attachment area for the interosseous membrane, which extends between the tibia and the fibula. The medial border commences below the medial condyle and terminates at the posterior border of the medial malleolus.

The portion of the tibia positioned between the anterior and medial borders is designated as the medial surface although it is positioned antero-medially. It forms the broad, subcutaneous portion of the tibia and provides attachment sites for multiple muscles and tendons of the leg. Between the anterior and lateral borders lies the lateral surface. At the proximal end this surface is situated laterally and continues in this orientation for the majority of its length. Beginning at the distal one-third of the shaft, this surface begins to twist slightly, finishing to face anteriorly. The posterior surface is located between the lateral and medial borders. It originates as a wide surface at the proximal end and tapers toward the ankle region. Positioned at the proximal end of the posterior surface is the popliteal line, a linear, roughened feature that runs infero-medially (Scheuer and Black, 2000). Approximately infero-laterally to the popliteal line is a hole, or nutrient foramen, that inserts distally into the bone and provides a path by which blood vessels may enter and supply nourishment to the bone. One foramen typically lies in the upper one-third of the posterior surface, but the location and number of foramina is known to vary between individuals (Scheuer and Black, 2000).

The Distal End

Again, as a result of position and function, the distal end of the tibia is easily differentiated from other skeletal elements (Figure 5). The distal end is "quadrilateral [in] shape" with the distinguishing medial malleolus extending inferiorly (Scheuer and Black, 2000).

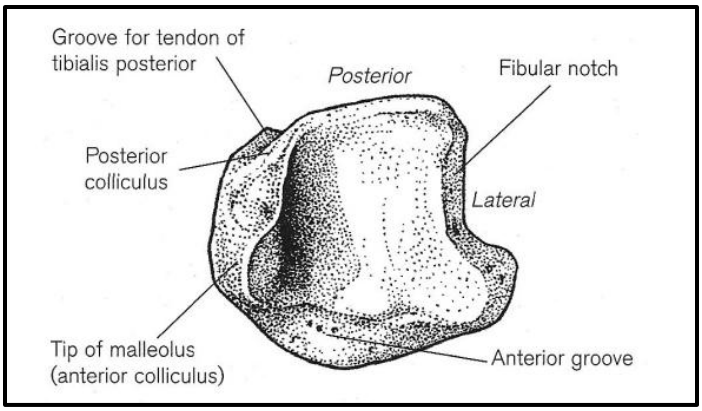

Figure 5. *Distal articular surface of right adult tibia. After Scheuer and Black 2000:404.*

The lateral surface of the shaft terminates as the anterior surface of the distal end. This smooth surface bulges slightly creating a distal end that is larger than the shaft. The medial malleolus is the thick extension of the shafts' medial surface, and like its predecessor, lies immediately below the skin. The posterior surface of the shaft divides into two surfaces creating the four-sided distal end. These include the posterior and lateral surface. An oblique groove is located on the medial edge of the posterior surface, and supplies a passageway for the tendon of the tibialis posterior. The fibular notch constitutes the entire lateral surface of the distal end. Also, the inferior portion of this end is an articular surface which creates a joint with the talus. This articulation continues onto the lateral wall of the medial malleolus.

Structures of the Leg

The fascia of the leg is responsible for creating the multiple compartments which include the muscles of the leg. The crural fascia is a deep fibrous, connective tissue that is attached to the anterior and medial borders of the tibia. Two intermuscular septa attach to the crural fascia and the fibula. The interosseous membrane, which extends between the interosseous crests of the bones of the legs, also unites with the intermuscular septa to partition the leg into its anterior, lateral, and posterior compartments. The sections of leg detailed above not only house muscles of the tibia, but also those arising from the fibula (Figure 6). The discussion in this section includes muscles affiliated with both long bones due to their correlating functions; a topic which will be discussed in further detail in a later section.

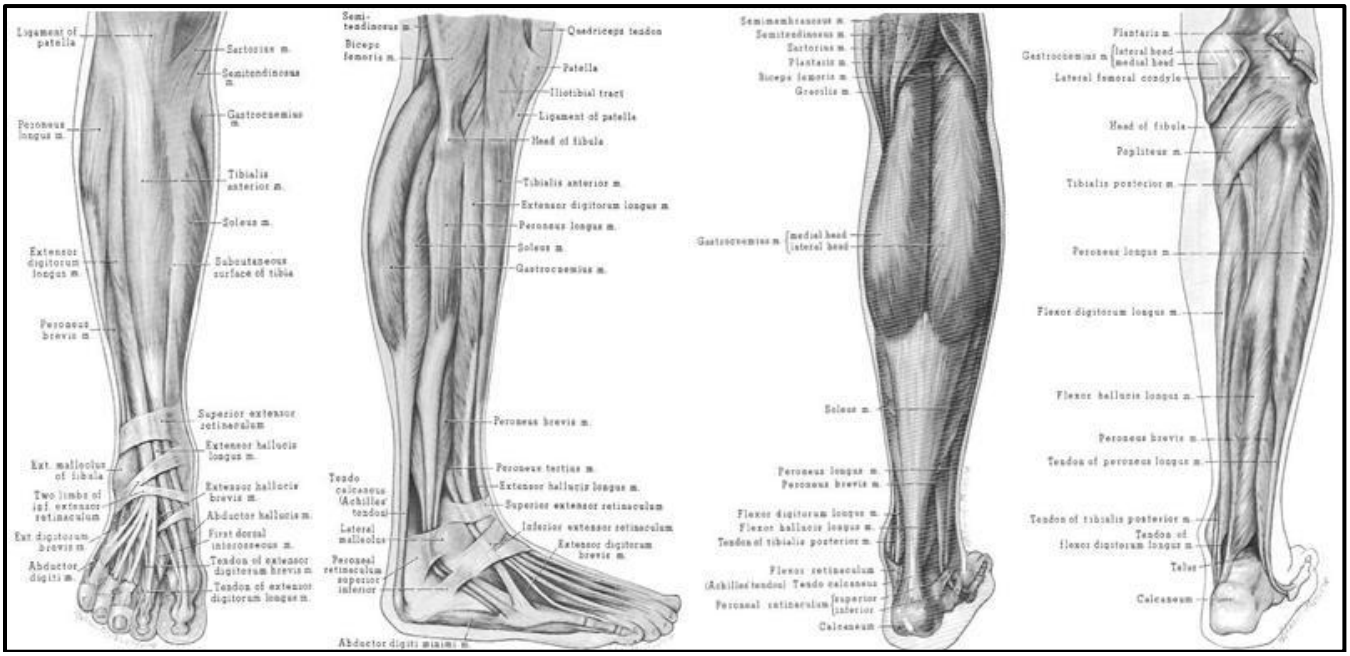

Figure 6. *Muscles of the leg. From left to right: Anterior view, lateral view, superficial posterior view, deep posterior view. After Jacob et al. 1978:193-198*

The anterior compartment contains four muscles, each functioning to mobilize the ankle as well as the foot. The tibialis anterior lies medial to the other muscles of this compartment and originates from the interosseous membrane and the lateral upper two-thirds of the tibia's shaft. Its tendon extends to the medial side of the foot to insert on the first cuneiform and the base of the first metatarsal. This affiliation with the toes allows it to invert the foot, while also acting to dorsiflex the ankle. The extensor digitorum longus also arises from the interosseous membrane, but originates from the anterior surface of the fibula. It inserts on the middle and distal phalanges of the second to fifth toes. Its actions include the extension of the toes, dorsiflexion of the ankle and eversion of the foot. The personeus tertius is a muscle that begins along the interosseous membrane and the distal fibula to insert on the fifth metatarsal, functioning to dorsiflex the ankle and evert the foot. The last muscle of the anterior compartment includes the exstensor hallucis longus. Its origin is the interosseous membrane and the middle half of the anterior fibula. Insertion occurs on the base of the distal phalanx of the big toe. It is responsible for both extending the big toe and dorsiflexion of the ankle.

The lateral compartment of the leg contains two muscles involved in the eversion of the foot, as well as the plantar flexion of the ankle. The peroneus longus is a superficial muscle that originates along the lateral surface and head of the fibula, descending to insert on the first cuneiform and the base of the first metatarsal. Origination of the peroneus brevis occurs along the lateral face of the shaft of the fibula. It inserts on the lateral side of the base of the fifth metatarsal.

The posterior compartment houses seven muscles which are designated as superficial and deep groups. The superficial group consists of the two muscles that, collectively, are referred to

as the calf (gastrocnemius and soleus). The gastrocnemius is a large, dual headed muscle that lies deep to the soleus, and originates on the lateral and medial epicondyles of the femur. The soleus originates from the soleal line of the tibia, the proximal-medial aspect of the tibia, and the proximal-posterior surface of the fibula. These muscles descend along the posterior surface of the leg to unite as one large tendon called the calcaneus or the Achilles tendon, which attaches to the calcaneus. The actions of gastrocnemius include the flexion of the leg and plantar flexion of the ankle. The soleus assists with plantar flexion of the ankle. Lying deep to these are the remaining five muscles of the posterior compartment. The plantaris is a small muscle of the leg that originates from the femur and inserts into the calcaneus tendon. Its function is considered insignificant and is not present in roughly 10% of humans. The popliteus muscle originates on the lateral condyle of the femur and wraps along the posterior surface of the proximal end of the leg to insert on the medial surface of the tibia. It functions as a flexor of the leg, as well as a medial rotator of the tibia. The tibialis posterior muscle arises from the interosseous membrane and along the posterior shaft of the fibula and the tibia. It descends to attach to multiple metatarsals and tarsals, involving it in the inversion of the foot and plantar flexion of the ankle. The last two muscles of the posterior compartment are responsible for the flexion of the phalanges. The flexor hallucis longus begins on the interosseous membrane and the lower two-thirds of the posterior surface of the fibula. Its tendon inserts on the base of the distal phalanx making it responsible for the flexion of the big toe. The network of tendons of the flexor digitorum longus flexes the remaining toes. Origination occurs along the posterior face of the tibia and the tendons of the muscle insert on underside of the distal phalanges of toes two through five (Carter, 2000).

The Knee Joint

As the largest joint in the human body, the knee is formed through the articulation of three bones: the distal end of the femur, the proximal end of the tibia and the patella, a sesamoid bone (bone encased within tendon) (Figure 1). It is a modified hinge joint which enables an increased range of motion to include "flexion and extension, medial and lateral rotation and gliding" (Carter, 2000). Several structures construct a firm foundation for this joint, while many muscles affiliated with the thigh and leg are responsible for mobilization of the joint; ultimately enabling particular movements associated with bipedal locomotion.

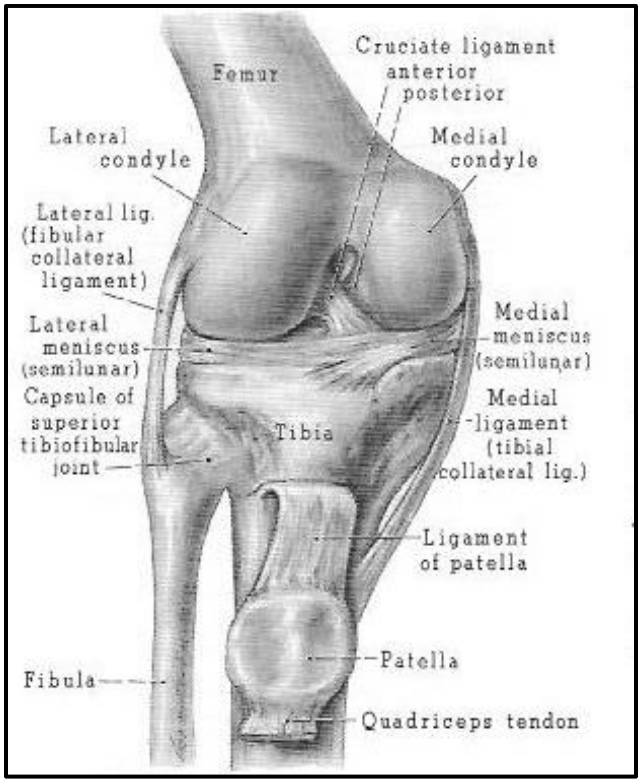

Figure 7. *Ligaments and cartilage of the knee. After Jacob et al. 1978:138.*

Multiple structures affiliated with the tibia are responsible for the stabilization of this joint (Figure 7). The collateral ligaments restrict "side-to-side" movement due to their position on the outer surface of the knee (Carter, 2000). The cruciate ligaments are located within the joint and attach to the anterior or posterior border of the intercondylar area, crossing each other to extend and attach to the inner surface of the femoral condyles. They both aid in securing the femur and tibia to one another. Individually, the cruciate ligaments have further responsibilities, but only the anterior cruciate ligament affects the integrity of the leg, while the other is solely responsible for stabilization of the femur. The placement of the anterior cruciate ligament allows it to protect against hyperextension of the leg (Carter, 2000). The cartilaginous structures of the knee, the medial and lateral menisci, offer further support of the joint. The medial meniscus is a relatively stationary structure that attaches directly to the proximal surface of the tibia. It functions to increase socket depth which helps to secure the medial femoral condyle within the joint. The lateral meniscus is "semicircular" in shape and also attaches to the proximal surface of the tibia (Jacob et al., 1978). Its attachment allows for minor gliding and produces a smooth surface for articulation with the lateral femoral condyle (Jacob et al., 1978).

Numerous muscles of the thigh originate on either the os coxae or femur and cross the knee joint to insert on the tibia (Figure 8). The position of these muscles enables them to produce the movements associated with this joint. The quadriceps femoris muscles are located on the anterior surface of the femur, and originate along the shaft of the femur as four individual muscles. They converge as the quadriceps tendon to insert into the patella and allow for the extension of the leg via the patellar tendon. Also located along the anterior aspect of the femur, the sartorious muscle originates on the superior iliac spine of the os coxa and courses down to insert on the medial surface of the tibia, slightly inferior to the tibial tuberosity. Crossing from the lateral border of the thigh to the medial border of the proximal tibia permits the muscle to aid in the flexion of the leg, as well as abduction (Jacobs et al., 1978). The hamstrings, which consist of three muscles of the posterior thigh (semitendinosus, biceps femoris, semimembranosus), are involved in flexing of the leg. The semitendinosus arises from the ischial tuberosity and is situated on the posterior-medial surface of thigh. The tendon of this muscle passes

posterior to the knee, turning anteriorly to insert along the medial surface of the proximal tibia. The biceps femoris begins as two heads, one originating along the linea aspera of the femur and the other at the ischial tuberosity. At approximately the lower third of the thigh the two heads unite.

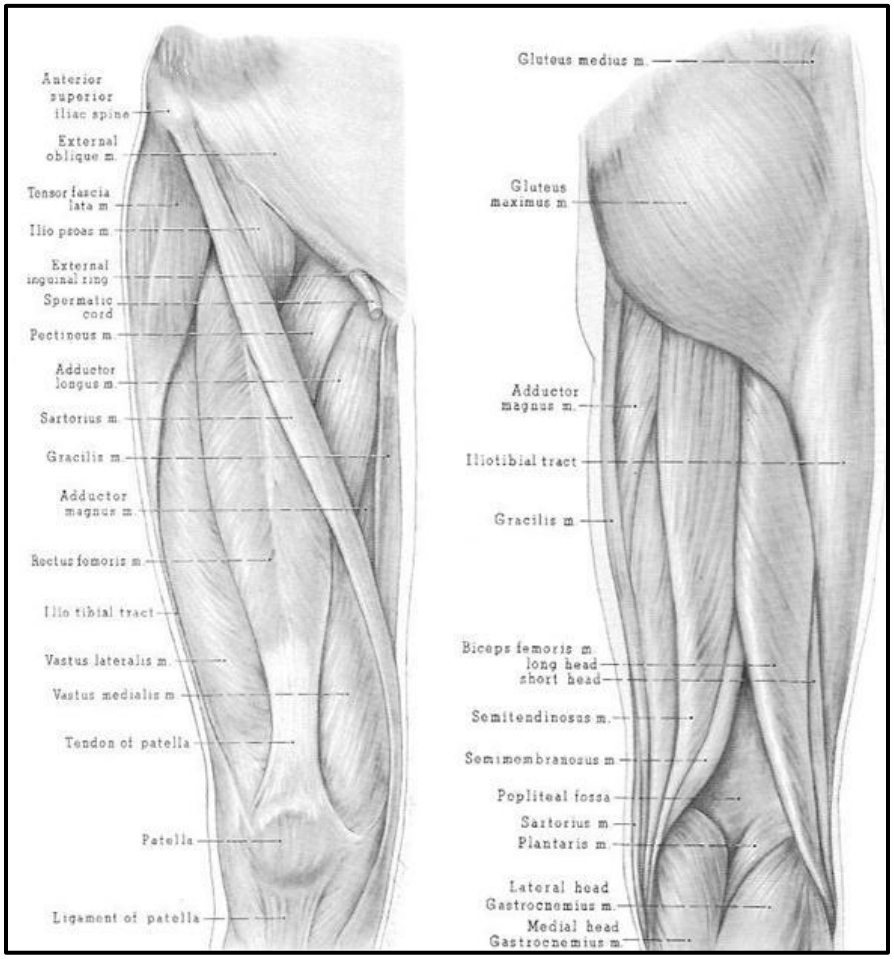

Figure 8. *Anterior (left) and posterior (right) views of the muscles of the thigh. After Jacob et al. 1978:188-189.*

The popliteus aids in flexion of the leg. The orientation of the muscle also permits its assistance in medial rotation of the leg. The gracilis muscle is located on the medial surface of the thigh. It begins along the anterior aspect of the os coxae and inserts on the medial surface of the proximal tibia just above the semitendinosus to further assist with flexion of the knee joint. The gastrocnemius, a muscle of the leg, also acts to produce flexion of the knee.

The Ankle Joint

The talocrural or ankle joint involves the articulations between the distal tibia and the talus, as well as the distal fibula and the talus. Through these articulations, the joint allows for "dorsiflexion (extension) and plantar flexion (flexion)" (Carter, 2000) (Figure 1). The eversion and inversion of the foot occur within joints of the tarsals and metatarsals; therefore they are not associated with the hinge movements of the ankle. The malleoli of the tibia and fibula create the prominences of the lower extremity commonly referred to as the ankle. They extend slightly past the talus on either side of the bone, impeding lateral or medial dislocation of the joint.

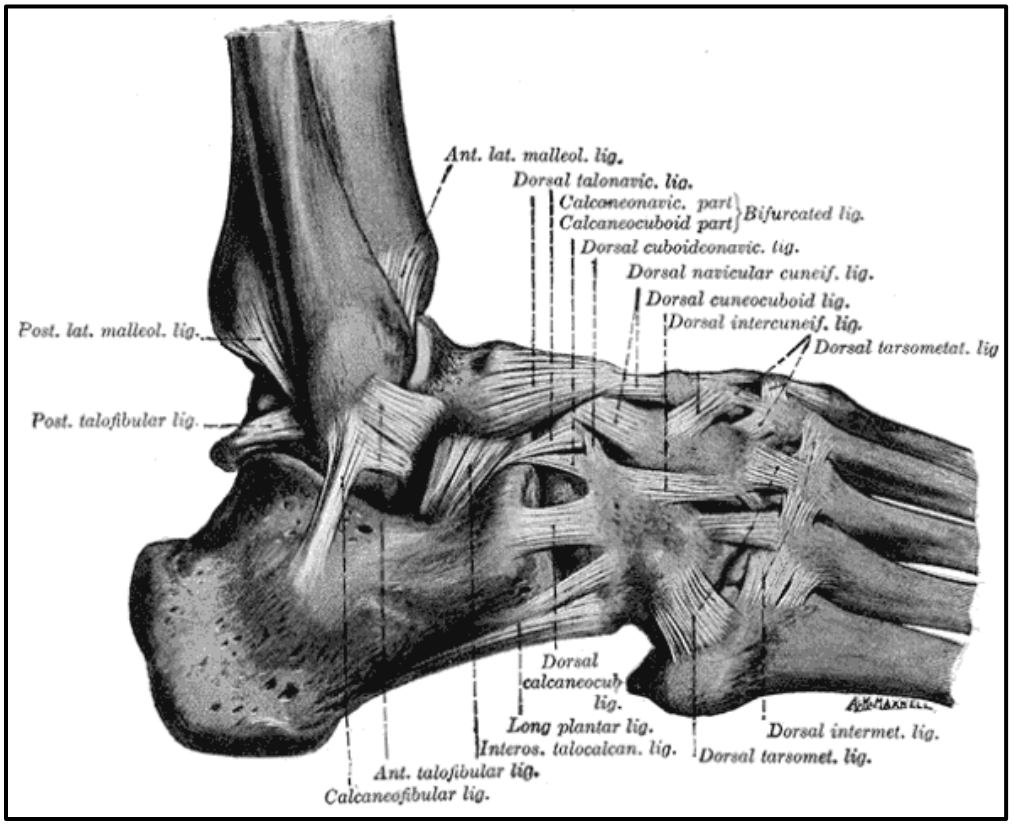

Figure 9. *Ligaments of the ankle. After Gray 2010 :284*

Like ligaments of the knee, those affiliated with the ankle strengthen the structure of the joint, while also restricting movements that result in displacement (Figure 9). The anterior and posterior tibiofibular ligaments extend between the tibia and fibula, respectively, securing the long bones to one another. The medial or deltoid ligament attaches to the medial malleolus of the tibia and stretches to attach to the talus, calcaneus, and navicular. It acts to bind the tibia to the medial side of the foot. The lateral ligament extends from the lateral malleolus of the fibula to attach to the talus and calcaneus, connecting the fibula and the foot. The location of these ligaments allows them to act concurrently to prevent backwards displacement of the talus, as well as aiding in stabilization of the ankle joint (Carter, 2000).

A large number of the muscles of the leg discussed above originate on either the tibia or fibula and are responsible for the mobilization of the ankle. The muscles of the anterior compartment of the leg are all responsible for aiding in dorsiflexion. Those of the lateral compartment are involved in plantar flexion. Of the seven muscles of the posterior compartment, three also assist in plantar flexion which includes the following muscles: the gastrocnemius, soleus, and tibialis posterior (Carter, 2000).

Age Related Changes

Growth and Development of the Human Skeleton

The human body undergoes an incremental process of development that results in the increased size and shape until finalization as its mature form. Generally, growth occurs at regular intervals, allowing these observed patterns to be utilized as indicators of age in the human skeleton. Variation in the rate and degree of growth and development exists among and between populations due to genetic and environmental influences. Pronounced differences are

observed between the sexes as well, where skeletal maturation is more advanced in females than males (Scheuer and Black, 2000).

Growth of skeletal elements occurs in three consecutive phases of development. The initial phase involves the appearance of the ossification center, generally taking place prenatally. Second, the centers begin to take on their unique morphological size and shapes. Once recognizable, age may be established based on the size of the element, or its stage of morphological development. Where appropriate, the final phase involves fusion of these centers. Fusion times are also indicative of skeletal age (Scheuer and Black, 2000).

Growth and Development of the Tibia

The first site of ossification, or bone formation, is designated as the primary center. The primary center of the tibia appears at approximately eight weeks in utero (Figure 10).

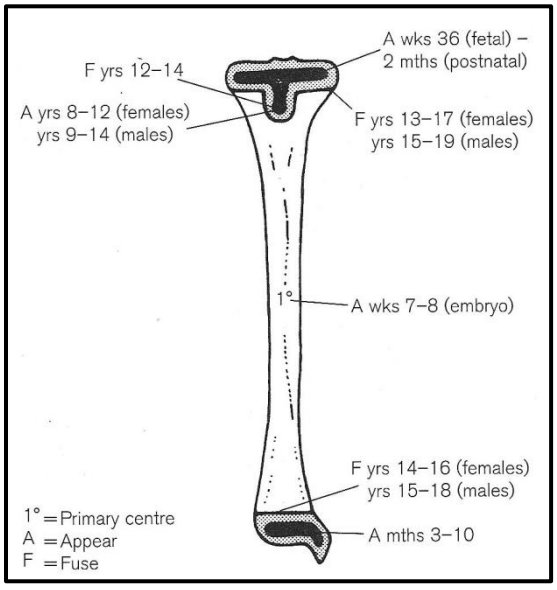

Figure 10. *Appearance and fusion times of the tibial ossification centers. After Scheuer and Black 2000:413.*

Ossification, or hardening, begins in the middle of the diaphysis, spreading outward towards the proximal and distal ends. Near week fourteen of fetal life the metaphyses, "an organized region of rapid growth (growth plate)," develops (Rang, 1969; Scheuer and Black, 2000). It is present in all long bones and is located between the diaphysis and epiphysis. The metaphysis is largely responsible for the linear growth of a long bone.

The formation and fusion of secondary centers occur at regular intervals allowing them to be applied as a form of age estimation for sub-adult individuals. The first to appear is the proximal epiphysis which does so shortly before birth and is present in roughly 80% of all full-term infants (Scheuer and Black, 2000). The postnatal development of the proximal epiphysis occurs at different rates in males and females; girls progress more quickly than boys. This begins as an advancement of just a few weeks at birth and increases to a two to three year advancement during adolescence. Fusion of the proximal epiphysis begins at thirteen years in females and fifteen and a half years in males, typically reaching completion by seventeen years in females and nineteen years in males. The proximal epiphysis accounts for roughly 57% of the tibia's overall length. The fusion of this epiphysis coincides with the completion of linear growth in the tibia. The secondary center for the tibial tuberosity appears between eight to twelve years in females and nine to fourteen years in males. Ossification begins distally and progresses proximally to cease at twelve to fourteen years.

The distal epiphysis is visible between three and ten months of age. At approximately eight and ten years the distal epiphysis begins to encase the distal portion of the shaft, while the medial malleolus is becoming discernible. In some cases the medial malleolus forms from a separate ossification center. Under these circumstances the center appears between seven and eight years in girls and between nine and ten years in boys, typically fusing two years following

appearance. Fusion of the distal epiphysis is complete within fourteen to sixteen years of age in females and fifteen to eighteen years in males.

Degenerative Age Related Changes

Following the completion of skeletal maturity, the human skeleton begins to undergo the natural biological process of bone degeneration. Throughout life the human skeleton experiences a highly complex, reoccurring process referred to as remodeling, where mature bone is resorbed and replaced with new bone as needed. Osteoclasts are bone cells responsible for the resorption of old bone. Conversely, osteoblasts are responsible for the "production and mineralization of the bone matrix" (Manolagas and Parfitt, 2010). The remodeling cycle has an average turnover of 10% per year in a healthy adult. As an individual ages this process becomes less efficient. Bone resporition begins to occur at a faster rate than bone production. Ultimately, this leads to a decrease in bone mass and bone strength (Manolagas and Parfitt, 2010).

The reduction of remodeling efficiency is a universal phenomenon in humans. However, the rate at which bone deformation occurs is variable among and between populations (Sevens and ViDarsdottir, 2008). Deformation is not only linked to inefficient remodeling, but is also impacted by the physical activity. The lower limbs are subjected to continuous biomechanical stresses associated with bipedal locomotion. Microdamage results from such normal wear and tear, and relies on the remodeling process to successfully repair damage. Studies demonstrate that when remodeling is suppressed or loading increases the amassing of microdamage diminishes bone strength and potentially results in "bone failure" (Drapeau and Streeter, 2006).

The knee joint, as a load bearing joint, is extremely susceptible this type of damage (Stevens and Vidarsdottir, 2008).

Cartilage also undergoes a universal aging process that further impacts bone deformation. Over the course of an individual's life "cartilage becomes softened and broken down" (Stevens and Vidarsdottir, 2008). Cartilage erosion is further heightened by chronic injuries or through enduring repetitive acute loading pressures. The diminution of cartilage in articulating surfaces eventually enables direct bone on bone contact, and is predominant in joints that experience the "greatest mechanical forces," such as the knee joint (Loeser, 2010). This eventually results in eburnation, the exposure of subchondral bone which causes the bone to take on a polished, ivory appearance. As direct contact continues, osteophytic lipping appears and can potentially lead to osteoarthritis (Stevens and Vidarsdottir, 2008).

Loeser and Shakoor (2003) describe osteoarthritis as "a prototypic aging-related disease" since it is by nature a disease whose prevalence increases with age and affects over half of the worlds elderly population. The previously discussed aging processes associated with the human skeleton increase an individual's risk of developing osteoarthritis. Joints suffering from osteoarthritis are characterized by common features including, but not limited to, articular cartilage degradation, thickening of subchondral bone and osteophytic lipping (Loeser, 2010). Alterations in bone morphology are rare in individuals younger than forty years of age. However, by the age of sixty, 80% of the world's population has osteoarthritis in at least one joint (Loeser and Shakoor, 2003). Of these individuals, 30% are affected in the knee, while the ankle is rarely affected (Loeser, 2010; Loeser and Shakoor, 2003).

Stevens and Vidarsdottir's 2008 study quantitatively assessed the degree of morphological variation in the human knee joint with increasing age. Results show that

significant differences in shape of the distal femur and proximal tibia exist between age groups. Their research demonstrates that in the United States osteoarthritis is more prevalent in males than females, but that, in the knee, little difference exists in the way in which the sexes age.

The degeneration of the human skeleton also impacts an individual's stature. Relethford and Lees (1981) use anthropometric data from an Irish population to evaluate the degree of statural loss with increasing age. Their study reveals stature declines as an individual ages. Statistically, men better represent this trend than women. They also found that statural loss is predominantly related to the compression of intervertebral discs throughout life, not degeneration associated with the lower extremity.

Sexual Dimorphism

Sexual dimorphism is simply the observable differences between the sexes of a particular species. In *Homo sapiens* this is represented in both the size and shape of the body. This morphological variation is reflective of the size and shape differences in the human skeleton. Overall, the "bones of males are longer, more robust, and display more rugged features than those of females" (Ubelaker, 1978). The disparity between males and females is minimal to non-existent in prepubescent individuals. Sex differences in the human skeleton become discernable following the initiation of physical and skeletal maturation, which is typically finalized by eighteen to twenty-three years of age (Scheuer and Black, 2000).

Sexual dimorphism is subject to spacial and temporal variation. A gradual reduction in the magnitude of sexual dimorphism has occurred over time. The fossil record demonstrates that early hominids were significantly more dimorphic than their modern counterparts (Frayer & Wolpoff, 1985). This is commonly attributed to an increase in the size of females throughout

time, inevitably decreasing the degree of morphological variation between the sexes (Gray & Wolfe, 1980). Discrepancies in morphology are also observed among and between populations. Genetic variability is the primary contributor to inconsistencies that exist within a population. Disparity in the degree of sexual dimorphism between populations is significantly impacted by differing environmental stressors which affect the growth and development of the human skeleton (Buffa et al., 2001).

Sexual dimorphism is also represented in human stature where males on average reach a greater height than females. Morphological variation between the sexes exists in lower limb length and the robusticity of these limbs. Studies show that sexual dimorphism in long bones is better represented by the circumference of the shaft rather than overall length of the bone (Iscan and Miller-Shaivitz, 1984; Holand, 1991; Safont et al., 2000). Holland (1991) found that the proximal end of the tibia is highly sexually dimorphic. Specifically, the biarticular breadth and the breadth of the medial and lateral condyles may be quantified to estimate the sex of an individual with significant degree of accuracy.

Research Concerning the Interaction of Stature and Skeletal Elements

Published literature that dates back over a century is reflective of the long existing interest in the correlation between living stature and human skeletal remains (Dwight, 1894, Pearson, 1899). Two methods are primarily employed in the "[reconstruction of] stature from skeletal remains: the anatomical method and regression equations" (Vercellotti et al., 2009). Throughout the years both methods have been subjected to testing and revisions by researchers. Of these methods, regression analyses are more commonly applied in bioarchaeological and forensic anthropological settings.

Anatomical Reconstruction

First developed by Thomas Dwight (1894) and later revised by Fully (1956), the anatomical method approximates stature by combining skeletal height (the sum of skeletal measurements known to contribute to overall living height) with an appropriate soft tissue constant. Studies by Raxter et al. (2006, 2007) further advanced this method through the refinement of measurements and soft tissue constants, as well as the addition of adjustments based on age changes affiliated with stature. These modifications boast high accuracy, producing estimates that are within 4.5 centimeters of the documented living stature in 95% of the individuals sampled by Raxter et al. (2006).

Regression Analysis

While the anatomical method provides more accurate estimates of stature, its applicability is limited due to its reliance on a complete skeleton (Vercellotti et al., 2009). When incomplete remains are present, researchers utilize regression techniques when reconstructing stature. The linear relationship that exists between long bone length and height has spurred the development of multiple regression equations specifically formulated from the dimensions of these bones. Prominent among such studies are Trotter and Glesser (1952,1958), whose efforts produced regression equations from the length of each individual long bone, as well as combinations of long bone lengths. When restricted to the use of individual long bones, results from their 1952 study indicate that the tibia provides the most accurate estimate of stature,

estimating living stature within three centimeters 70% of the time. Coupling the tibia and femur, they were able to develop equations that yield estimates with 79% accuracy. Data from Trotter and Glesser's (1958) continued research indicates different regression equations are necessary to precisely estimate the stature of different group affiliations due to the close affiliation of stature and genetic factors and environmental factors, such as nutrition, disease, and social status.

Fragmentary Remains as Indicators of Stature

The majority of regression techniques necessitate the presence of complete skeletal elements for a more precise application; however, the fragmentary nature of remains in archaeological and forensic settings makes this difficult (Holland, 1992). Muller (1935) pioneered work to circumvent this issue by estimating total bone length from fragmentary long bones. She defined segments of the humerus, radius and tibia, using them to "[calculate] the percentage of total length represented by each section," which were subsequently used to approximate the length of the three long bones (Wright and Vásquez, 2003).

Building on this method Steele and Mckern (1969) and Steele (1970) generated regression equations that estimate maximum long bone length from defined segments of remains. The resulting value is then used in the appropriate regression equation formulated by Trotter and Glesser (1952, 1958). Steele (1970) developed regression formulae to approximate total length from single measurements, as well as combinations of measurements. This technique involves the calculation of two estimates, thereby increasing standard error. He also provided equations that used combinations of measurements to directly estimate stature. These equations resulted in larger standard errors than those affiliated with Trotter and Glesser (1952, 1958). Despite the

increased standard error associated with his "two-step method," Steele (1970) advocates this method over the latter until modern samples are fully evaluated.

A study undertaken by Jacobs (1992) uses two lower limb bones, the femur and the tibia, to evaluate the applicability of Steele's (1970) techniques on a prehistoric European sample. Results show that Steele's equations do not accurately estimate total length in this sample. Further inquest demonstrated that segment lengths defined by Steele correlated significantly with bone length in the population. Jacobs used these correlations to produce population-specific formulae, thus supporting Steele's methodology. He explains that bone proportions of the two samples differed, and suggests that the measurements defined by Steele include areas of the bone that are "sensitive to activity pattern and intensity, as expressed in degree of muscularation" (Jacobs, 1992). Jacobs concurs with Steele's advisement that the sample from which regression equations are devised must have congruent activity patterns with the population under study.

The Tibia as an Indicator of Stature

Research on the relationship of long bone length and stature consistently produce data that demonstrates a stronger correlation exists between lower limb bones than those of the upper limbs (Meadows and Jantz, 1995; Jantz and Jantz, 1999). Of the three long bones of the lower extremity, multiple recent studies have focused on correlations between the tibia and height (Holland, 1992; Jacobs, 1992; Nath et al., 1998; Duyar and Pelin, 2003). In many cases, research on this topic was an endeavor to test or revise previously published regression techniques.

Holland (1992) confined his study to measurements of the proximal tibia, establishing linear regression formulae that estimate stature with standard errors that match or are less than those of Trotter and Glesser (1952, 1958) and Steele and McKern (1969). Unfortunately, application of this method could prove difficult since the proximal and distal ends of long bones are commonly damaged in both bioarchaeological and forensic settings. The author also recommends this method be a last resort due to a small test sample size.

Another study assessed significance of linear, sagittal and transverse measurements of the tibia as indicators of stature (Nathe et al., 1998). Data from an all male, Indian sample suggests that of the measurements taken, the sagittal measurement exhibits the highest correlation to stature. The second highest correlations were found among the transverse measurements, while the linear measurements demonstrated the least significant correlations. Further research is necessary to test the validity of sagittal dimensions producing "the best statural estimates" since only one sagittal measurement was defined by this study.

Research by Duyar and Pelin (2003) used the tibia to ascertain whether a population's body proportions impacted the applicability of a regression equation if it was not developed from a sample demonstrating similar proportions. Results support the common opinion that group specific regression formulae are needed for accurate and precise stature reconstruction.

Temporal Variation and Secular Effects

Secular change is an alternative form of variation that, "like senescence and other biological-based morphological variations," alters the human skeleton over time (Voisin, 2011). Secular variation is a non-genetic response to sociocultural and environmental pressures that is

represented in skeletal morphology over successive generations. These alterations may stem from either human plasticity or microevolotionary changes (Moore-Jansen, 1989).

Observations of human populations demonstrate that secular variation affects individuals at varying degrees. Research indicates that exposure to environmental pressures that may lead to modifications in morphology begin in utero, and have their most profound influence from six months and three years of age. A noticeable impact on skeletal morphology may be witnessed by the onset of childhood, but will not necessarily be represented by each individual to the same degree. The sexes typically display secular variation at different intensities, where males are affected more than females (Jantz and Jantz, 1999). Disparities are also found between populations of differing socioeconomic levels, meaning technological improvements likely lead to improved nutrition and medical conditions which influences secular trend (Releford and Lees, 1981).

A common method of assessing secular trends has been to evaluate the temporal change in stature within and among populations. This has occurred due to the close affiliation between stature and economic and nutritional factors. As a result, studies on skeletal samples seeking to evaluate the degree of secular variation tend to focus on the size and shape of long bones. In particular, the long bones of the lower extremity exhibit positive allometry with stature, therefore when stature fluctuates, the bones remain proportionate in length (Meadows and Jantz, 1995). A study such as this was undertaken by Jantz and Jantz (1999), attests to the efficiency of long bones as indicators of secular variation, and suggests their use when stature data is unavailable. Results support previous claims by Meadows and Jantz (1995) that, concerning the extremities, distal bones (e.g. tibia and fibula) are more reflective of a secular trend than proximal bones (e.g.

femur). This means distal bones will be more reflective of secular variation; therefore the proportions between stature and long bone length are more likely to remain constant.

In an effort to minimize the impact of secular variation in this study, where possible, the sample has been restricted to individuals born within a ten year range. This precaution is undertaken to control the amount of morphological variation the sample reflects as a result of exposure to sociocultural and environmental pressures over time. It is also an effort to control the proportionality of stature and tibiae size and shape within the sample.

CHAPTER THREE

MATERIALS AND METHODS

Introduction

Prior to implementing this study a detailed protocol concerning data collection and analysis was developed in order to ensure the success of this research. In an effort to enable the replication of the procedures set out by this study, this chapter details the sampling, measurement and statistical protocol, while also providing insight into the osteological collection from which the sample was derived.

History of the Hamann-Todd Osteological Collection

Originally located at Western Reserve Medical School, the Hamann-Todd Osteological Collection was initialized by anatomy professor, Dr. Carl August Hamann in 1893. He was succeeded by Dr. T. Wingate Todd in 1912, who is responsible for amassing the majority of the complete human skeletal remains in the collection. In 1951 the collection began the transition to its current resting place, and is now housed in the Cleveland Museum of Natural History in Cleveland, Ohio (İşcan, 1990; Jones-Kern and Latimer, 1996).

Thus far, the collection consists of approximately 3,100 human remains with birth years ranging from 1825 to 1910, as well as nearly 900 non-human primate specimens. All of the human specimens are of donated origins, most becoming a part of the collection as a result of a law stipulating local, unclaimed cadavers be donated to the collection with the expectations of being utilized for investigative and educational purposes (de la Cova, 2011). This process allowed for the documentation of age at death, sex, group affiliation, cause of death, anthropomorphic measurements, and when possible, living stature and the donation source (de la

Cova, 2011; İşcan, 1990; Kelley and El-Najjar, 1980). In most cases, Todd examined the cadavers before and after autopsies, at which point he identified any pathological lesions and abnormalities associated with the specimens, including, but not limited to, evidence of healed fractures, degenerative changes, dietary deficiencies, and disease (Kelley and El-Najjar, 1980). Cadaver weight and height were also obtained through a process of suspending the specimens from the auditory canal by ice tongs, where height was measured with a "graduated wooden-staff" (Cobb, 1932).

As is the nature of anatomical collections, the Hamman-Todd Osteological Collection possesses inherent limitations primarily due to the manner of acquisition and selection criteria utilized in choosing donated specimens. Consequently, the collection is not representative of the general population. Dominated by unclaimed cadavers, the remains predominantly represent a common socioeconomic background of "poor working class" Americans of the late 1800s to the early 1900s (de la Cova, 2011). Each of the specimens is designated as either Black or White, and are individuals who have died in or around Cleveland, Ohio, but were not necessarily born in the region (Todd and Lindala, 1928). The collection contains specimens from a variety of states. In most cases they are first generation Americans, where White individuals are natives of Northern states and Black individuals of Southern states. The inclusion of Southern Blacks is attributed to the migration of migrants following their emancipation.

The collection is also comprised of all age groups, from neonate to elderly. While it is beneficial to researchers for the collection to be comprised of all age groups, this poorly represents the population of the time, suggesting that age at death was evenly distributed when, in fact, life expectancy of the time was between 20 and 40 years of age. Remains were often selected for pathological lesions present on the skeletal elements. In these cases, the individuals

are considered the "most robust, or healthiest" of the populations due to their survival of a particular disease long enough to develop lesions (de la Cova, 2011).

Evidence of disease or nutritional deficiency is prevalent within the collection, and those impacting the integrity of the tibia are discussed here. Multiple infectious diseases exist within the collection, accurately depicting the prebiotic period and creating a unique opportunity to study the effect of such diseases on skeletal elements, as well as medical treatments of the time (Jones-Kern and Latimer, 1996). Tuberculosis, usually manifesting itself in the spine and the metaphyses and joints of long bones, is represented in high frequency among specimens, especially amid the Black group affiliation. This is consistent with historical data, which reports higher rates of tuberculosis among African Americans, likely due to extensive environmental pressures associated with slavery and the Great Migration (de la Cova, 2011). Treponematosis is also in high occurrence, which commonly produces inflammation of the periosteum. The shape of the tibia is often compromised by this type of infection, creating a 'saber-shin' appearance, characterized by an "unusual anterior bowing and sharp anterior margins" (Ubelaker, 1978). Healed evidence of rickets, a systemic disease involving the inadequate intake of vitamin D during childhood, is observed within the collection. It impacts the long bones of the lower limb by producing pronounced bowing of the diaphysis, reducing the transverse diameter of the bone and increasing the antero-posterior diameter (Ortner, 2003). All specimens displaying skeletal malformation, such as that which results from pathological or nutritional stressors were eliminated from the study.

The Study Sample

The sample utilized in this study consisted of measurements from 382 American Black specimens of known age, sex, group affiliation and cadaver height. Measurements were collected from both sexes; 202 males and 180 females. Of the 202 males, 102 were 40 years of age or younger and 100 were older than 40 years of age. The females included 91 individuals 40 years of age or under and 89 exceeding 40 years of age.

The specimens were restricted to skeletally mature individuals with complete tibiae. In order to minimize interference with bone dimensions, specimens exhibiting pathological conditions, nutritional deficiencies or any form of post-mortem damage were excluded from the sample. In order to account for secular change the specimens were restricted to a birth range of ten years, but, unfortunately, due to a limited number of American Blacks in the collection and associated effects of disease and poor nutrition on the tibiae, this was not possible throughout the entire sample. Only males 40 years of age or younger remained within the ten year birth range. The birth range of older adult males was increased to include individuals born within twelve years, and that of the young adult females was increased to a range of fifteen years. The Hamann-Todd specimens comprising the older adult Black females included the least number of individuals, requiring the birth year restriction to be completely lifted in order to maximize the number of tibial measurements obtained.

Measurement Protocol

The standard measurement protocol implemented in this study was developed at the Wichita State University Biological Anthropology Laboratory. The sample is comprised of

traditional and non-traditional measurements (refer to Appendix A for measurement descriptions), and were employed with standard osteometric instruments, including the following: an osteometric board, Mitutoyo digimatic calipers, and fiberglass tape. Where possible, the left tibia was measured. In cases where the left tibia was absent or damaged, dimensions were obtained from the right tibia. Initially, all measurements were recorded in millimeters to the nearest tenth on Data Collection Forms (Appendix B) and then later entered into an Excel spreadsheet.

Traditional Measurements

This study includes six traditional measurements of the tibia, each recorded according to guidelines defined by Moore-Jansen et al. (1994). Of these, three require the use of an osteometric board and consists of the following: length of the tibia, maximum epiphyseal breadth of the proximal tibia, and maximum epiphyseal breadth of the distal tibia. Two of the measurements were taken using digital sliding calipers. These measurements include the maximum diameter and transverse diameter of the tibia at the nutrient foramen. The remaining measurement, the circumference of the tibia at the nutrient foramen, was taken with a fiberglass tape.

Non-Traditional Measurements

Six non-traditional measurements were developed for application in the present study. Each of the measurements made use of the standard equipment discussed above. Two of the

dimensions, the maximum length of the tibia and the anterior/posterior epiphyseal breadth of the distal tibia, were taken with the osteometric board. Digital sliding calipers were used to collect three of the measurements; the maximum diameter of the tibia at the midshaft, the transverse diameter of the tibia at the midshaft, and the length from the intercondylar eminence to the nutrient foramen. Finally, the circumference of the tibia at the midshaft is acquired through the use of a fiberglass tape.

Statistical Procedures and Analysis

As a means to evaluate the manner by which the tibia varies and the morphological variation represented by the tibial measurements of this study, as well as the relationship between the dimensions and cadaver height, univariate and several multivariate statistical procedures were implemented. Univariate statistics were applied to the individual measurements to establish the means, standard deviation, variance and ranges of each. This method was specifically utilized to evaluate the degree of sexual dimorphism inherent within the sample, as well as the effects of age on this variation.

Table 1. Calibration and test samples

Sample Title	Calibration (n)	Test (n)
Pooled Black sample	240	142
Female Black sample	120	60
Male Black sample	120	82
Young adult Black sample	120	73
Young adult female Black sample	60	31
Young adult male Black sample	60	42
Older adult Black sample	120	69
Older adult female Black sample	60	29
Older adult male Black sample	60	40

All multivariate analyses were performed using the Statistical Analysis System (SAS) (SAS Statistical Institute Inc, 1985; 1999; Delwiche and Slaughter, 2008), which included the PROC CORR, PROC STEPWISE, PROC DISCRIM, and PROC REG procedures. In order to apply these analyses, multiple calibration samples were developed, along with corresponding test samples (Table 1). These subsamples were utilized with the appropriate statistical application.

Morphological Variation Among and Between the Sexes and Their Respective Age Groups

The PROC CORR procedure was applied in order to assess whether the tibial measurements used in this study covary, and if so, to what degree. SAS implements the Pearson product moment correlation in this procedure in order to quantify the strength and direction that the variables correlate (SAS Statistical Institute Inc, 1985; 1999; Delwiche and Slaughter, 2008). The correlation coefficient is the measure of the degree of linear correlation between two values, in this case, two measurements. Its values range from -1 to +1, where (-) represents a negative linear relationship and (+) a positive linear relationship. The closer this coefficient is to one, the stronger the correlation between the two variables. The correlation coefficients were distinguished as significant at <.05. The samples utilized to perform this evaluation consisted of the pooled, female, male, young adult female, young adult male, older adult female and older adult male samples.

In order to further assess the impact of sex and age on the sample, a multivariate analysis of variance was applied. A PROC STEPWISE was performed with a MAXR option to distinguish the optimal discrimination model, with the requirement that the model and individual variables be significant at <.05 (SAS Statistical Institute Inc, 1985; 1999; Delwiche and

Slaughter, 2008). This procedure aids in the determination of the twelve variables' capabilities to discriminate sex from the size and shape of the tibia, individually and in group. A PROC DISCRIM was subsequently applied to the observations developed through the previous procedure to identify the classification rates produced by the stepwise models (SAS Statistical Institute Inc, 1985; 1999; Delwiche and Slaughter, 2008). These procedures were initially performed on the derived calibration samples to produce the discriminating models and to investigate the reliability of these models to correctly classify based on the sex of the individual. In order to further evaluate the reliability of these variables to discriminate based on sex, a PROC DISCRIM was performed for each independent test sample. These calibration and test samples involved in these procedures included the pooled sample, the young adult sample, and the older adult sample.

The Interaction of Stature and Tibial Morphology

In order to assess the relationship between cadaver height and the tibial dimensions, the PROC REG procedure was implemented (SAS Statistical Institute Inc, 1985; 1999; Delwiche and Slaughter, 2008). Each measurement was evaluated separately in an effort to establish the degree to which the tibial dimensions may explain the variation in cadaver height, therefore indicating which may enable the prediction of living stature. The significance level for this procedure is set at <.05. This procedure was applied to seven calibration samples which included the pooled sample, the female sample, the male sample, the young adult female sample, the young adult male sample, the older adult female sample, and the older adult male sample to ensure the affects of age and sex on the interaction were thoroughly investigated.

Intra-Observer Error

The potential and reliability of this study could be greatly impacted by the replicability of the measurements employed during data collection. In order to assess the reliability and consistency of the measurement protocol, intra-observer error was evaluated. Eight individuals performed the twelve measurements associated with this study in accordance with the measurement protocol (Appendix B). The dimensions collected by these individuals demonstrate that variation among the measurements is minor (<3.00%), suggesting that any variation within this sample is expected to be the result of biological and cultural factors, rather than replicability issues (Droessler, 1981). Further testing of intra-observer error with a larger sample size is recommended should the measurements presented in this study be utilized elsewhere.

CHAPTER FOUR

RESULTS

Summary Statistics

The morphological variation among and between the sexes and age groups of the tibial dimensions is demonstrated by the summary statistics. All results in the summary statistics are recorded in millimeters and rounded to the nearest tenth of a millimeter. The univariate summary statistics for each of the samples is located in the appendix (Appendix C).

The summary statistics demonstrates consistently larger means for all measurements in the male sample than that of the female sample (Table 2). The greatest difference in size and shape is represented by the maximum length of the tibia (MLT), the length of the tibia (L0T), the length from intercondylar eminence to the nutrient foramen (LIN), the circumference of the tibia at the nutrient foramen (C0N), and the circumference of the tibia at the midshaft (C0M), where the male and female means are separated by a minimum of ten millimeters. The greatest degree of distribution is also represented by these measurements in both males and females. For both groups, the maximum length of the tibia (MLT) and the length of the tibia (L0T) demonstrate the greatest spread of the dimensions associated with this study, followed by the length from intercondylar eminence to the nutrient foramen (LIN).

The trends associated with the pooled female and male samples remain constant when the samples are evaluated based on sex, as well as their corresponding age groups (Tables 3 and 4). The morphology represented by the measurements for young and older males is routinely larger than those of the young and older females, respectively. The greatest discrepancies between the corresponding age groups of the sexes are represented by the same measurements discussed above.

Table 2. Summary Statistics – Pooled sample

		Males n = 202		Females n = 180	
Code	**Measurement**	**Mean**	**St. Dev.**	**Mean**	**St. Dev.**
MLT	Maximum length of the tibia	402.6	23.8	368.3	23.5
L0T	Length of the tibia	393.6	22.7	359.0	23.2
MEP	Maximum epiphyseal breadth of the proximal tibia	79.9	3.7	70.8	3.7
MED	Maximum epiphyseal breadth of the distal tibia	50.0	3.9	44.1	2.8
AED	Anterior/Posterior epiphyseal breadth of the distal tibia	42.2	3.0	37.5	2.4
MDN	Maximum diameter of the tibia at the nutrient foramen	35.7	3.3	31.4	2.4
TDN	Transverse diameter of the tibia at the nutrient foramen	26.3	2.5	23.2	2.3
MDM	Maximum diameter of the tibia at the midshaft	30.9	2.9	26.8	2.7
TDM	Transverse diameter of the tibia at the midshaft	23.5	2.6	20.7	2.6
LIN	Length from intercondylar eminence to the nutrient foramen	126.2	12.0	113.6	11.8
C0N	Circumference of the tibia at the nutrient foramen	98.8	7.1	87.4	6.1
C0M	Circumference of the tibia at the midshaft	87.0	6.7	76.9	5.2

Table 3. Summary Statistics –Male sample

		≤ 40 years of age n = 102		> 40 years of age n = 100	
Code	**Measurement**	**Mean**	**St. Dev.**	**Mean**	**St. Dev.**
MLT	Maximum length of the tibia	401.2	23.3	403.7	24.4
L0T	Length of the tibia	392.9	22.6	394.1	23.0
MEP	Maximum epiphyseal breadth of the proximal tibia	79.4	3.6	80.4	3.9
MED	Maximum epiphyseal breadth of the distal tibia	50.0	4.4	50.0	3.4
AED	Anterior/Posterior epiphyseal breadth of the distal tibia	41.8	2.5	42.6	3.5
MDN	Maximum diameter of the tibia at the nutrient foramen	35.2	3.0	36.1	3.5
TDN	Transverse diameter of the tibia at the nutrient foramen	26.3	2.3	26.2	2.8
MDM	Maximum diameter of the tibia at the midshaft	30.6	2.8	31.3	3.1
TDM	Transverse diameter of the tibia at the midshaft	23.3	2.5	23.6	2.7
LIN	Length from intercondylar eminence to the nutrient foramen	126.7	13.1	125.5	10.9
C0N	Circumference of the tibia at the nutrient foramen	98.0	6.9	99.7	7.1
C0M	Circumference of the tibia at the midshaft	86.2	5.5	87.9	7.7

Table 4. Summary Statistics – Female sample

		≤ 40 years of age n = 91		> 40 years of age n = 89	
Code	**Measurement**	**Mean**	**St. Dev.**	**Mean**	**St. Dev.**
MLT	Maximum length of the tibia	370.2	21.5	366.2	25.2
L0T	Length of the tibia	361.1	23.8	357.0	22.4
MEP	Maximum epiphyseal breadth of the proximal tibia	69.9	3.4	71.7	3.8
MED	Maximum epiphyseal breadth of the distal tibia	43.5	2.5	44.7	3.0
AED	Anterior/Posterior epiphyseal breadth of the distal tibia	37.2	2.4	37.8	2.4
MDN	Maximum diameter of the tibia at the nutrient foramen	31.0	2.4	31.7	2.4
TDN	Transverse diameter of the tibia at the nutrient foramen	23.3	2.5	23.0	2.1
MDM	Maximum diameter of the tibia at the midshaft	26.8	2.1	26.8	3.3
TDM	Transverse diameter of the tibia at the midshaft	20.2	2.1	21.1	2.9
LIN	Length from intercondylar eminence to the nutrient foramen	113.6	11.6	113.6	12.1
C0N	Circumference of the tibia at the nutrient foramen	86.8	6.0	88.1	6.0
C0M	Circumference of the tibia at the midshaft	76.1	4.8	77.8	5.4

The summary statistics for the dimensions of the male tibia show slight variations between the age groups within the sample (Table 3). Each of the means for the measurements, excluding the maximum epiphyseal breadth of the distal tibia (MED), the transverse diameter at the nutrient foramen (TDN) and the length from the intercondylar eminence to the nutrient foramen (LIN), exhibit a trend for the slight enlargement of the size and shape of the tibia as age increases. The means of the maximum epiphyseal breadth of the distal tibia (MED) is the same for both male age groups, while the transverse diameter at the nutrient foramen (TDN) and the length from the intercondylar eminence to the nutrient foramen (LIN) express minor reductions in the means. The distributions of these dimensions exhibit a similar pattern as the majority of the means. The spread from the mean increases from the young adult age groups to the older adult age groups in all the dimensions except the length from the intercondylar eminence to the nutrient foramen (LIN), which decreases by 2.2 millimeters.

Among the female sample, the variation between the dimension means of the age groups is irregular (Table 4). Seven of the measurements enlarge as age progresses. These include the maximum epiphyseal breadth of the proximal tibia (MEP), the maximum epiphyseal breadth of the distal tibia (MED), the anterior/posterior epiphyseal breadth of the distal tibia (AED), the maximum diameter of the tibia at the midshaft (MDN), the transverse diameter of the tibia at the midshaft (TDM), the circumference of the tibia at the nutrient foramen (C0N), and the circumference of the tibia at the midshaft (COM). The maximum length of the tibia (MLT), the length of the tibia (L0T), and the transverse diameter of the tibia at the nutrient foramen (TDN) demonstrate a slight reduction in the mean with increasing age. Two of the measurements, the maximum diameter at the midshaft (MDM) and the length from the intercondylar eminence to

the nutrient foramen (LIN), remain the same, showing no fluctuation in the mean between the younger adult and older adult age groups.

Irregularities are also expressed in the distribution of the dimensions between the age groups of the female sample. Primarily, the distribution of the values increases as age increases. The spread of the dimensions enlarges in the maximum length of the tibia (MLT), the maximum epiphyseal breadth of the proximal tibia (MEP), the maximum epiphyseal breadth of the distal tibia (MED), the maximum diameter of the tibia at the nutrient foramen (MDN), the transverse diameter of the tibia at the midshaft (TDM), the length from the intercondylar eminence to the nutrient foramen (LIN), and the circumference of the tibia at the midshaft (C0M). The variability associated with the dimensions of the anterior/posterior epiphyseal breadth of the distal tibia (AED), the maximum diameter of the tibia at the nutrient foramen (MDN), and the circumference of the tibia at the nutrient foramen (C0M) remains constant between the two age groups. The spread of the values associated with the length of the tibia (LOT) and the transverse diameter of the tibia at the nutrient foramen (TDN) reduces slightly with increasing age.

Size and Shape Variation of the Tibia

The PROC CORR procedure was performed as a means of evaluating the relationships between dimensions of the tibia. Analyzing the covariance of the measurements associated with this study reveals whether a linear relationship exists between these dimensions, as well as the strength and direction of the relationship. This procedure required the use of seven calibration samples and their corresponding test samples to include the following: the pooled sample, the female sample, the male sample, the young adult female sample, the young adult male sample, the older adult female sample, and the older adult male sample. These samples were selected so

that the impact of an individual's age and/or sex on the relationship of the tibial dimensions could also be assessed.

A combination of PROC STEPWISE and PROC DISCRIM procedures were performed to assess the degree to which the tibial measurements represent the size and shape variation that exists within and between males and females, as well as the respective age groups of the specimens. The PROC STEPWISE procedure with the MAXR criterion was applied to the dimensions of the pooled, young adult, and older adult calibration samples to establish the optimal sex discriminating models for each. Classification rates were then discerned for each calibration sample, as well as the test samples through the application of a PROC DISCRIM procedure. These procedures were undertaken in order to assess the degree to which sexual dimorphism and age related skeletal alterations is represented by the tibial measurements.

Covariance of Tibial Dimensions

The PROC CORR procedure demonstrates the way in which the size and shape of the tibia covaries as represented by the tibial dimensions collected in this study. This statistical procedure was first applied to the calibration samples (Tables 5-11) to establish the way in which variables correlate and to what degree. The same evaluation was applied to the test samples to verify the consistency of the findings (Refer to Appendix D for test sample correlation results). Tables 5 through 11 present the data affiliated with the Pearson product moment correlations, where the values above the diagonal (1.0000) represent the correlation coefficients and the values below represents the probability associated with the correlations. In order to concisely address the relationships illustrated by this procedure, the correlations will be discussed in

reference to the areas or features of the tibia being quantified. Otherwise noted, each of the correlations presented are significant at <.05. Only those relationships that are consistent, barring minor fluctuations, between the calibration sample and the test sample will be presented here.

Within the pooled calibration sample the strongest correlation is represented between the maximum length of the tibia (MLT) and the length of the tibia (LOT) with a correlation coefficient of 0.9952 (Table 5). Those variables concerning the distal and proximal end correlate highly among this sample as well. The relationship between the maximum epiphyseal breadth of the proximal tibia (MEP) and the maximum epiphyseal breadth of the distal tibia (MED) is represented by an r-value of 0.8222, which is the next highest correlation associated with this calibration sample. The maximum epiphyseal breadth of the proximal tibia (MEP) and the anterior/posterior epiphyseal breadth of the distal tibia (AED) are correlated at 0.7899. Multiple dimensions concerning the diaphysis of the tibia also express strong correlations. Of the midshaft measurements, the relationship between the maximum diameter of the tibia at the midshaft (MDM) and the circumference of the tibia at the midshaft (C0M) constitutes the strongest correlation and is represented by an r-value of 0.7365. Those regarding the dimensions at the level of the nutrient foramen that exhibit the highest correlations are the maximum diameter of the tibia at the nutrient foramen (MDN) and the circumference of the tibia at the nutrient foramen (C0N) with a correlation coefficient of 0.8839, as well as the transverse diameter of the tibia at the nutrient foramen (TDN) and the circumference of the tibia at the nutrient foramen (C0N) with a coefficient of 0.7806. Strong correlations concerning the midshaft and the nutrient foramen also occur. The circumference of the tibia at the nutrient foramen (C0N) demonstrates an r-value of 0.7920 with the circumference of the tibia at the

midshaft (C0M) and an r-vaule of 0.7966 with the maximum diameter of the tibia at the midshaft (MDM). The maximum diameter of the tibia at the nutrient foramen (MDN) is found to correlate with the circumference of the tibia at the midshaft (C0M) at 0.7552, as well as with the maximum diameter of the tibia at the midshaft (MDM) at 0.7539. Lastly, a strong correlation is represented by the relationship between the maximum epiphyseal breadth of the proximal tibia (MEP) and the circumference of the tibia at the nutrient foramen (C0N) with an r-value of 0.7994.

Table 5. Pearson product moment correlations between tibial measurements in the pooled calibration sample

	MLT	L0T	MEP	MED	AED	MDN	TDN	MDM	TDM	LIN	C0N	C0M
MLT	1.0000	0.9952	0.6965	0.6235	0.6548	0.6108	0.5444	0.5996	0.5636	0.6609	0.6701	0.6348
L0T	<.0001	1.0000	0.6888	0.6198	0.6518	0.6052	0.5357	0.5939	0.5578	0.6607	0.6615	0.6263
MEP	<.0001	<.0001	1.0000	0.8222	0.7899	0.7161	0.6249	0.7324	0.5483	0.4396	0.7994	0.7323
MED	<.0001	<.0001	<.0001	1.0000	0.7215	0.6430	0.4970	0.6822	0.4830	0.3937	0.7260	0.6560
AED	<.0001	<.0001	<.0001	<.0001	1.0000	0.7169	0.5885	0.6358	0.5192	0.4292	0.7252	0.6550
MDN	<.0001	<.0001	<.0001	<.0001	<.0001	1.0000	0.6287	0.7539	0.5425	0.2211	0.8839	0.7552
TDN	<.0001	<.0001	<.0001	<.0001	<.0001	<.0001	1.0000	0.4981	0.6791	0.2867	0.7806	0.6567
MDM	<.0001	<.0001	<.0001	<.0001	<.0001	<.0001	<.0001	1.0000	0.3603	0.3576	0.7966	0.7365
TDM	<.0001	<.0001	<.0001	<.0001	<.0001	<.0001	<.0001	0.0041	1.0000	0.4942	0.6375	0.6441
LIN	<.0001	<.0001	<.0001	<.0001	<.0001	0.0006	<.0001	<.0001	<.0001	1.0000	0.2793	0.4208
C0N	<.0001	<.0001	<.0001	<.0001	<.0001	<.0001	<.0001	<.0001	<.0001	<.0001	1.0000	0.7920
C0M	<.0001	<.0001	<.0001	<.0001	<.0001	<.0001	<.0001	<.0001	<.0001	<.0001	<.0001	1.0000

Values are significant at $\alpha < .05$

When correlation levels are evaluated for the female calibration sample the highest correlation is 0.9926 and is exhibited by the relationship between the maximum length of the tibia (MLT) and the length of the tibia (L0T) (Table 6). A correlation is expressed by each of the dimensions of the proximal and distal ends of the tibia. This relationship is between the maximum epiphyseal breadth of the proximal tibia (MEP) and the maximum epiphyseal breadth of the distal tibia (MED), as well as the between the maximum epiphyseal breadth of the proximal tibia (MEP) and the anterior/posterior epiphyseal breadth of the distal tibia (AED). The correlation rates of these associations are 0.6480 and 0.6019, respectively. The maximum

epiphyseal breadth of the distal tibia (MED) is also correlated with the anterior/posterior epiphyseal breadth of the distal tibia (AED) with an r-value of 0.6092.

Table 6. Pearson product moment correlations between tibial measurements in the female calibration sample

	MLT	L0T	MEP	MED	AED	MDN	TDN	MDM	TDM	LIN	C0N	C0M
MLT	1.0000	0.9926	0.3330	0.3949	0.4019	0.3072	0.3264	0.2166	0.4174	0.5713	0.3862	0.4154
L0T	<.0001	1.0000	0.3089	0.3711	0.3854	0.2944	0.3147	0.1992	0.4067	0.5685	0.3715	0.3937
MEP	0.0002	0.0006	1.0000	0.6480	0.6019	0.5391	0.4788	0.4345	0.4181	0.1403	0.6566	0.6412
MED	<.0001	<.0001	<.0001	1.0000	0.6092	0.4450	0.3315	0.2911	0.3330	0.2269	0.4910	0.4984
AED	<.0001	<.0001	<.0001	<.0001	1.0000	0.5267	0.4951	0.2140	0.4462	0.2089	0.5412	0.5404
MDN	0.0006	0.0011	<.0001	<.0001	<.0001	1.0000	0.4722	0.5712	0.4151	-0.0636	0.8034	0.6905
TDN	0.0003	0.0005	<.0001	0.0002	<.0001	<.0001	1.0000	0.2611	0.5573	0.0762	0.7274	0.5866
MDM	0.0175	0.0292	<.0001	0.0013	0.0189	<.0001	0.0040	1.0000	-0.0503	0.0352	0.6103	0.5306
TDM	<.0001	<.0001	<.0001	0.0002	<.0001	<.0001	<.0001	0.5852	1.0000	0.3557	0.4467	0.6170
LIN	<.0001	<.0001	0.1264	0.0127	0.0220	0.0636	0.4082	0.7031	<.0001	1.0000	-0.0192	0.2347
C0N	<.0001	<.0001	<.0001	<.0001	<.0001	<.0001	<.0001	<.0001	<.0001	0.8353	1.0000	0.7207
C0M	<.0001	<.0001	<.0001	<.0001	<.0001	<.0001	<.0001	<.0001	<.0001	0.0099	<.0001	1.0000

Values are significant at $\alpha < .05$

The diaphyseal dimensions of the transverse diameter of the midshaft (TDM) and the circumference of the midshaft (C0M) covary, displaying a correlation coefficient of 0.6170. A high correlation is expressed between the maximum diameter of the tibia at the nutrient foramen (MDN) and the circumference of the tibia at the nutrient foramen (C0N) with a 0.8304 r-value. The transverse diameter of the tibia at the nutrient foramen (TDN) and the circumference of the tibia at the nutrient foramen (C0N) correlate at a value of 0.7274. Like the pooled sample, the measurements of the midshaft and the nutrient foramen correlate among one another. These consist of relationships between the circumference of the tibia at the nutrient foramen (C0N) and the maximum diameter of the tibia at the midshaft (MDM) correlating at 0.6103, the maximum diameter of the tibia at the nutrient foramen (MDN) and the circumference of the tibia at the midshaft (C0M) correlating at 0.6905, as well as the circumference of the tibia at the nutrient foramen (C0N) and the circumference of the tibia at the midshaft (C0M), correlating at 0.7207. Further, high correlations are expressed at 0.6566 between the maximum epiphyseal breadth of

the proximal tibia (MEP) and the circumference of the tibia at the nutrient foramen (C0N). The maximum epiphyseal breadth of the proximal tibia (MEP) correlates with the circumference of the tibia at the midshaft (C0M) with an r-value of 0.6412.

As was with the previous two calibration samples, the correlation that is the strongest within the male calibration sample (Table 7) is exhibited by the relationship between the maximum length of the tibia (MLT) and the length of the tibia (L0T). This is represented by an r-value of 0.9920. Of those measurements that quantify the shape of the shaft of the tibia, four high correlations exist. These include measurements at the level of the nutrient foramen between the maximum diameter of the tibia at the nutrient foramen (MDN) and the circumference of the tibia at the nutrient foramen (C0N), as well as between the transverse diameter of the tibia at the nutrient foramen (TDN) and the circumference of the tibia at the nutrient foramen (C0N). These relationships achieve r-values of 0.8153 and 0.6048, respectively. The maximum diameter of the tibia at the midshaft (MDM) correlates with both the circumference of the tibia at the nutrient foramen (C0N) at 0.6764 and the maximum diameter of the tibia at the nutrient foramen (MDN) at 0.6191.

Table 7. Pearson product moment correlations between tibial measurements in the male calibration sample

	MLT	L0T	MEP	MED	AED	MDN	TDN	MDM	TDM	LIN	C0N	C0M
MLT	1.0000	0.9920	0.5649	0.3050	0.4404	0.4504	0.3055	0.4854	0.3722	0.5361	0.5148	0.4017
L0T	<.0001	1.0000	0.5487	0.3065	0.4412	0.4405	0.2874	0.4793	0.3646	0.5380	0.4960	0.3894
MEP	<.0001	<.0001	1.0000	0.5519	0.5292	0.4297	0.2554	0.5168	0.2237	0.1910	0.5337	0.3484
MED	0.0007	0.0007	<.0001	1.0000	0.3572	0.3171	0.0509	0.5102	0.1564	0.0505	0.4631	0.2762
AED	<.0001	<.0001	<.0001	<.0001	1.0000	0.5124	0.2301	0.4774	0.1849	0.1955	0.4626	0.2876
MDN	<.0001	<.0001	<.0001	0.0004	<.0001	1.0000	0.4151	0.6191	0.3283	-0.0721	0.8153	0.5387
TDN	0.0007	0.0015	0.0049	0.5809	0.0115	<.0001	1.0000	0.1870	0.5805	0.0417	0.6048	0.3905
MDM	<.0001	<.0001	<.0001	<.0001	<.0001	<.0001	0.0408	1.0000	0.2208	0.1871	0.6764	0.5714
TDM	<.0001	<.0001	0.0140	0.0881	0.0432	0.0003	<.0001	0.0154	1.0000	0.3701	0.5334	0.4265
LIN	<.0001	<.0001	0.0367	0.5835	0.0324	0.4342	0.6511	0.0408	<.0001	1.0000	-0.0203	0.1792
C0N	<.0001	<.0001	<.0001	<.0001	<.0001	<.0001	<.0001	<.0001	<.0001	0.8255	1.0000	0.5785
C0M	<.0001	<.0001	<.0001	0.0023	0.0014	<.0001	<.0001	<.0001	<.0001	0.0502	<.0001	1.0000

Values are significant at $\alpha < .05$

The correlation procedures, when preformed on the young adult female calibration sample, reveal numerous highly correlated dimensions of the tibia (Table 8). The strongest relationship is between the association of the maximum length of the tibia (MLT) and the length of the tibia (L0T) with a correlation coefficient of 0.9936. The dimensions of the proximal and distal tibia that express the strongest covariance are the maximum epiphyseal breadth of the proximal tibia (MEP) and the maximum epiphyseal breadth of the distal tibia (MED) which is represented by a r-value of 0.6156.

Table 8. Pearson product moment correlations between tibial measurements in the young adult female calibration sample

	MLT	L0T	MEP	MED	AED	MDN	TDN	MDM	TDM	LIN	C0N	C0M
MLT	1.0000	0.9936	0.5115	0.4643	0.5623	0.5085	0.4204	0.4808	0.5432	0.5186	0.5648	0.6427
L0T	<.0001	1.0000	0.5223	0.4662	0.5728	0.4995	0.4246	0.4707	0.5482	0.5319	0.5623	0.6438
MEP	<.0001	<.0001	1.0000	0.6156	0.5907	0.5757	0.4989	0.4560	0.4847	0.0075	0.6419	0.5958
MED	0.0002	0.0002	<.0001	1.0000	0.6427	0.4705	0.3537	0.3245	0.2166	0.1456	0.4812	0.4682
AED	<.0001	<.0001	<.0001	<.0001	1.0000	0.5033	0.4886	0.3978	0.3504	0.2204	0.6166	0.5866
MDN	<.0001	<.0001	<.0001	0.0001	<.0001	1.0000	0.4033	0.7457	0.4781	-0.1593	0.8454	0.7720
TDN	0.0008	0.0007	<.0001	0.0056	<.0001	0.0014	1.0000	0.3917	0.6314	0.0460	0.7373	0.7027
MDM	0.0001	0.0001	0.0003	0.0114	0.0016	<.0001	0.0020	1.0000	0.3659	0.0213	0.7200	0.8146
TDM	<.0001	<.0001	<.0001	0.0964	0.0061	0.0001	<.0001	0.0040	1.0000	0.2794	0.5804	0.7154
LIN	<.0001	<.0001	0.9548	0.2670	0.0907	0.2242	0.7271	0.8720	0.0307	1.0000	-0.1236	0.1782
C0N	<.0001	<.0001	<.0001	<.0001	<.0001	<.0001	<.0001	<.0001	<.0001	0.3468	1.0000	0.8601
C0M	<.0001	<.0001	<.0001	0.0002	<.0001	<.0001	<.0001	<.0001	<.0001	0.1730	<.0001	1.0000

Values are significant at $\alpha < .05$

Multiple dimensions associated with the shaft of the tibia are characterized by strong correlations as well. Those taken at the nutrient foramen involves the association between the circumference of the tibia at the nutrient foramen (C0N) and the maximum diameter of the tibia at the nutrient foramen (MDN), a relationship that expresses a coefficient of 0.8454. The circumference of the tibia at the nutrient foramen (C0N) also correlates well with the transverse diameter of the tibia at the nutrient foramen (TDN). This relationship displays an r-value of 0.7373. The circumference of the tibia at the midshaft (C0M) expresses high covariance with the transverse diameter of the tibia at the midshaft (TDM) at 0.7154 and the maximum diameter of the tibia at

the midshaft (MDM) at 0.8146. The dimensions of the midshaft and nutrient foramen also correlate among one another. A correlation coefficient of 0.6314 is exhibited by the transverse diameter of the tibia at the nutrient foramen (TDN) and the transverse diameter of the tibia at the midshaft (TDM). The maximum diameter of the tibia at the midshaft (MDM) and the circumference of the tibia at the nutrient foramen (C0N) correlate at 0.7200.

The young adult male calibration sample was evaluated for correlations among the tibial dimensions (Table 9), revealing the strongest correlation to be between the maximum length of the tibia (MLT) and the length of the tibia (L0T). This association is characterized by a correlation coefficient of 0.9930.

Table 9. Pearson product moment correlations between tibial measurements in the young adult male calibration sample

	MLT	L0T	MEP	MED	AED	MDN	TDN	MDM	TDM	LIN	C0N	C0M
MLT	1.0000	0.9930	0.4242	0.1130	0.3293	0.3940	0.3530	0.3464	0.3997	0.6387	0.4363	0.4738
L0T	<.0001	1.0000	0.4223	0.1240	0.3350	0.3955	0.3355	0.3570	0.4017	0.6400	0.4279	0.4686
MEP	0.0007	0.0008	1.0000	0.4712	0.5394	0.2960	0.2267	0.4330	0.1919	0.2944	0.3711	0.4409
MED	0.3899	0.3454	0.0001	1.0000	0.4063	0.3640	0.0626	0.3935	0.1825	0.1005	0.3988	0.3774
AED	0.0102	0.0089	<.0001	0.0013	1.0000	0.5256	0.2576	0.5845	0.3283	0.2595	0.5209	0.6213
MDN	0.0018	0.0018	0.0217	0.0043	<.0001	1.0000	0.4555	0.6709	0.3072	-0.0543	0.8968	0.7563
TDN	0.0057	0.0088	0.0816	0.6346	0.0469	0.0003	1.0000	0.2826	0.5853	-0.0030	0.7057	0.5779
MDM	0.0067	0.0051	0.0005	0.0019	<.0001	<.0001	0.0287	1.0000	0.2055	0.2383	0.6423	0.8061
TDM	0.0016	0.0015	0.1418	0.1627	0.0104	0.0170	<.0001	0.1153	1.0000	0.3670	0.4361	0.5608
LIN	<.0001	<.0001	0.0224	0.4451	0.0452	0.6803	0.9820	0.0667	0.0039	1.0000	-0.0396	0.2975
C0N	0.005	0.0006	0.0035	0.0016	<.0001	<.0001	<.0001	<.0001	0.0005	0.7640	1.0000	0.8109
C0M	0.0001	0.0002	0.0004	0.0030	<.0001	<.0001	<.0001	<.0001	<.0001	0.0210	<.0001	1.0000

Values are significant at $\alpha < .05$

Multiple correlations were displayed in reference to the dimensions of the diaphysis. Those involving the nutrient foramen consisted of relationships between the circumference of the tibia at the nutrient foramen (C0N) and the transverse diameter of the tibia at the nutrient foramen (TDN) with an r-value of 0.7057, as well as the circumference of the tibia at the nutrient foramen (C0N) and the maximum diameter of the tibia at the nutrient foramen (MDN) with an r-value of 0.8968. The circumference of the tibia at the midshaft (C0M) correlates highly with the

maximum diameter of the tibia at the midshaft (MDM), expressing a correlation coefficient of 0.8061. The maximum diameter of the tibia at the midshaft (MDM) also correlates strongly with both the maximum diameter of the tibia at the nutrient foramen (MDN) and the circumference of the tibia at the nutrient foramen (C0N). These correlations are represented by the r-values 0.6709 and 0.6423, respectively. The length from the intercondylar eminence to the nutrient foramen (LIN) correlates closely with two dimensions. These are the maximum length of the tibia (MLT) at 0.6387 and the length of the tibia (L0T) at 0.6400.

The strongest correlation expressed by the older adult female calibration sample (Table 10) involves the maximum length of the tibia (MLT) and the length of the tibia (L0T), with a correlation coefficient of 0.9919. The covariance of the proximal and distal ends are represented by the maximum epiphyseal breadth of the proximal tibia (MEP) and its association with the maximum epiphyseal breadth of the distal tibia (MED) with a correlation rate of 0.6650 and the anterior/posterior epiphyseal breadth of the distal tibia (AEP) with a correlation rate of 0.6013.

Table 10. Pearson product moment correlations between tibial measurements in the older adult female calibration sample

	MLT	L0T	MEP	MED	AED	MDN	TDN	MDM	TDM	LIN	C0N	C0M
MLT	1.0000	0.9919	0.2234	0.3763	0.3053	0.1356	0.2011	0.1454	0.3693	0.6328	0.2202	0.2633
L0T	<.0001	1.0000	0.1750	0.3347	0.2725	0.1267	0.1732	-0.0041	0.3513	0.6167	0.2000	0.2300
MEP	0.0864	0.1811	1.0000	0.6650	0.6013	0.4929	0.5282	0.4511	0.3577	0.2591	0.6863	0.6677
MED	0.0030	0.0090	<.0001	1.0000	0.5724	0.4122	0.3565	0.2846	0.3994	0.2946	0.5066	0.5081
AED	0.0177	0.0351	<.0001	0.5724	1.0000	0.5450	0.5599	0.0998	0.5000	0.1968	0.4780	0.4902
MDN	0.3017	0.3348	<.0001	0.0011	<.0001	1.0000	0.6007	0.4503	0.3675	0.0266	0.7592	0.6086
TDN	0.1234	0.1857	<.0001	0.0052	<.0001	<.0001	1.0000	0.1377	0.5665	0.1214	0.7365	0.5207
MDM	0.9122	0.9752	0.0003	0.0275	0.4479	0.0003	0.2940	1.0000	-0.2848	0.0481	0.5347	0.3490
TDM	0.0037	0.0059	0.0050	0.0016	<.0001	0.0039	<.0001	0.0274	1.0000	0.4123	0.3555	0.5452
LIN	<.0001	<.0001	0.0456	0.0223	0.1317	0.8399	0.3554	0.7150	0.3103	1.0000	0.0838	0.2818
C0N	0.0909	0.1256	<.0001	<.0001	0.0001	<.0001	<.0001	<.0001	0.4771	0.5242	1.0000	0.5955
C0M	0.0421	0.0770	<.0001	<.0001	<.0001	<.0001	<.0001	0.0063	0.4257	0.0292	<.0001	1.0000

Values are significant at $\alpha < .05$

Those measurements quantifying the diaphysis at the nutrient foramen that correlate highly involve a relationship with the circumference of the tibia at the nutrient foramen (C0N) and two

other dimensions. These include the maximum diameter of the tibia at the nutrient foramen (MDN), possessing a correlation coefficient of 0.7592, and the transverse diameter of the tibia at the nutrient foramen (TDN) with a coefficient of 0.7365. The maximum diameter of the tibia at the nutrient foramen (MDN) correlates with the circumference of the tibia at the midshaft (C0M). Their correlation rate is 0.6086. The length from the intercondylar eminence to the nutrient foramen's (LIN) relationship with the maximum length of the tibia (MLT) correlates at 0.6328. The relationship between the length from the intercondylar eminence to the nutrient foramen (LIN) and the length of the tibia (L0T) displays an r-value of 0.6167. Lastly, the relationship between the maximum epiphyseal breadth of the proximal tibia (MEP) and the circumference of the tibia at the nutrient foramen (C0N) produces a correlation coefficient of 0.6863.

When evaluated for covariance, the highest correlation coefficient in the older adult male calibration sample is expressed through the relationship of the maximum length of the tibia (MLT) and the length of the tibia (L0T) with an r-value of 0.9918 (Table 11). Separately, these measurements also both provide a high correlation with the maximum epiphyseal breadth of the proximal tibia (MEP). The maximum epiphyseal breadth of the proximal tibia (MEP) produces a correlation coefficient of 0.6568 with the maximum length of the tibia (MLT) and a coefficient of 0.6320 with the length of the tibia (L0T). The covariance of the distal and proximal end is demonstrated by the correlation of the maximum epiphyseal breadth of the proximal tibia (MEP) and the maximum epiphyseal breadth of the distal tibia (MED) through an r-value of 0.6233. The circumference of the tibia at the nutrient foramen (C0N) correlates with multiple tibial dimensions. These include the maximum epiphyseal breadth of the proximal tibia (MEP), the maximum diameter of the tibia at the nutrient foramen (MDN) and the transverse diameter of the

tibia at the midshaft (TDM). The respective correlation coefficients are 0.6185, 0.7663, and 0.6355.

Table 11. Pearson product moment correlations between tibial measurements in the older adult male calibration sample

	MLT	L0T	MEP	MED	AED	MDN	TDN	MDM	TDM	LIN	C0N	C0M
MLT	1.0000	0.9918	0.6568	0.4694	0.5051	0.4801	0.2857	0.5999	0.3573	0.4658	0.5643	0.3682
L0T	<.0001	1.0000	0.6320	0.4586	0.5049	0.4664	0.2638	0.5828	0.3385	0.4638	0.5396	0.3539
MEP	<.0001	<.0001	1.0000	0.6233	0.5118	0.4832	0.2879	0.5705	0.2652	0.1399	0.6185	0.2980
MED	0.0002	0.002	<.0001	1.0000	0.3409	0.3002	0.0421	0.6334	0.1316	-0.0057	0.5196	0.2363
AED	<.0001	<.0001	<.0001	0.007	1.0000	0.4906	0.2311	0.4009	0.1023	0.1895	0.4204	0.1429
MDN	0.0001	0.0002	<.0001	0.0198	<.0001	1.0000	0.4162	0.5792	0.3705	-0.0625	0.7663	0.4411
TDN	0.0269	0.0417	0.0257	0.7494	0.0756	0.0009	1.0000	0.1362	0.5870	0.0751	0.5622	0.3234
MDM	<.0001	<.0001	<.0001	<.0001	0.0015	<.0001	0.2993	1.0000	0.2526	0.1697	0.7012	0.4551
TDM	0.0051	0.0082	0.0405	0.3162	0.4367	0.0036	0.5870	0.0515	1.0000	0.3739	0.6355	0.3820
LIN	0.0002	0.0002	0.2864	0.9654	0.1470	0.6350	0.5687	0.1948	0.0033	1.0000	0.0205	0.1386
C0N	<.0001	<.0001	<.0001	<.0001	0.0008	<.0001	<.0001	<.0001	<.0001	0.8764	1.0000	0.4725
C0M	0.0038	0.0055	0.0207	0.0692	0.2762	0.004	0.0117	0.0003	0.0026	0.2911	0.0001	1.0000

Values are significant at $\alpha < .05$

Morphological Variation Between Males and Females

The PROC STEPWISE procedure with the MAXR option was applied to dimensions of the tibia in the pooled Black sample, which included both sexes and age groups. Five discriminating models were produced through this process, with an associated R-squared value that increases slightly with each subsequent model (Table 12). Each model has an overall model probability of <.0001. Four of the five models also maintains a partial probability of <.05 for each variable. The maximum epiphyseal breadth of the proximal tibia is the only measurement represented in each model developed from this particular calibration sample. The last model produced and presented was the five-variable model of step five. While the R-square expressed minimal increase in successive steps, the partial probability of multiple variables began to exceeded <.05, and therefore were eliminated as possible indicators of sex.

Table 12. Stepwise models for the pooled calibration sample

Step	Variables	R^2	Model F	Partial F	P
1	Maximum epiphyseal breadth of the proximal tibia	0.6420	426.82	426.82	<.0001
2	Maximum epiphyseal breadth of the proximal tibia	0.6542	224.20	91.14	<.0001
	Maximum Epiphyseal breadth of the distal tibia			8.37	0.0042
3	Maximum epiphyseal breadth of the proximal tibia	0.6619	154.00	79.14	<.0001
	Maximum epiphyseal breadth of the distal tibia			7.66	0.0061
	Length from intercondylar eminence to the nutrient foramen			5.36	0.0215
4	Maximum epiphyseal breadth of the proximal tibia	0.6675	117.93	52.62	<.0001
	Maximum epiphyseal breadth of the distal tibia			8.18	0.0046
	Transverse diameter of the tibia at the nutrient foramen			3.94	0.0482
	Length from intercondylar eminence to the nutrient foramen			5.24	0.0229
5	Maximum epiphyseal breadth of the proximal tibia	0.6697	94.89	41.25	<.0001
	Maximum epiphyseal breadth of the distal tibia			6.46	0.0117
	Transverse diameter of the tibia at the nutrient foramen			3.51	0.0621
	Maximum diameter of the tibia at the midshaft			1.58	0.2099
	Length from intercondylar eminence to the nutrient foramen			4.99	0.0264

All measurements are significant to $\alpha = .05$

The best single-variable model (Table 13) in the pooled sample was identified as the maximum epiphyseal breadth of the proximal tibia (MEP). This model has an R-squared value of 0.6420 and an F-value of 426.82. In reference to the calibration sample, sex is correctly estimated in males 90.00% of the time and 93.33% of the time in females, boasting an overall classification rate of 91.66%. The test sample exemplifies slightly lower classification rates. This model correctly identified 85.37% of males and 86.67% of females, overall, correctly identifying the sex of 85.92% of the specimens.

The second model is a two-variable model (Table 14) which combines the maximum epiphyseal breadth of the proximal tibia (MEP) and the maximum epiphyseal breadth of the distal tibia (MED), creating a model with an R-squared value of 0.6542 and an F-value of 224.20. This model appropriately classifies 88.33% of the males and 90.83% of the females in the pooled sample, with an overall correct classification of 89.58%. Application to the pooled

test sample once again resulted in a minimal decrease in the classification rates. Between the sexes, 87.80% of the males and 86.67% of the females were correctly designated. Overall, 87.32% of the test sample was accurately identified as the appropriate sex.

Table 13. Classification rates for step 1 model for the pooled sample

	Calibration Sample			Test Sample	
	Male	Female		Male	Female
Male	108/120	12/120	Male	70/82	12/82
	90.00%	10.00%		85.37%	14.63%
Female	8/120	112/120	Female	8/60	52/60
	6.67%	93.33%		13.33%	86.67%
Total	220/240		Total	122/142	
Correct	91.66%		Correct	85.92%	

Table 14. Classification rates for step 2 model for the pooled sample

	Calibration Sample			Test Sample	
	Male	Female		Male	Female
Male	106/120	14/120	Male	72/82	10/82
	88.33%	11.67%		87.80%	12.20%
Female	11/120	109/120	Female	8/60	52/60
	9.17%	90.83%		13.33%	86.67%
Total	215/240		Total	124/142	
Correct	89.58%		Correct	87.32%	

The next model consisted of three variables, the two measurements of the preceding step, the maximum epiphyseal breadth of the proximal tibia (MEP) and the maximum epiphyseal breadth of the distal tibia (MED), in addition to the length from the intercondylar eminence to the nutrient foramen (LIN) (Table 15). An R-squared value of 0.6619 and an F-value of 154.00 are associated with this three-variable model. When this model is applied to the calibration sample, the males are correctly identified 88.33% of the time and the females 92.50% of the time, resulting in an overall classification rate of 90.42%. When applied to an independent test

sample, a classification accuracy of 87.80% in males and 83.67% in females is achieved, while overall correct classification of 87.32%.

Table 15. Classification rates for step 3 model for the pooled sample

	Calibration Sample			Test Sample	
	Male	Female		Male	Female
Male	106/120 88.33%	14/120 11.67%	Male	72/82 87.80%	10/82 12.20%
Female	9/120 7.50%	111/120 92.50%	Female	8/60 13.33%	52/60 83.67%
Total Correct	217/240 90.42%		Total Correct	124/240 87.32%	

The fourth model produced from the pooled sample involves four variables including the maximum epiphyseal breadth of the proximal tibia (MEP), the maximum epiphyseal breadth of the distal tibia (MED), the transverse diameter of the tibia at the nutrient foramen (TDN), and the length from the intercondylar eminence to the nutrient foramen (LIN) (Table 16). The model displays an R-squared value of 0.6675 and an F value 117.93. Males are correctly classified with 89.17% accuracy and females with 92.50% accuracy. The overall correct classification of the calibration sample is 90.83%. Correct classification occurs in 89.02% of males and 88.33% of females in the test sample, with an overall value of 88.73%. These values are again, slightly lower than the results of the calibration sample.

Table 16. Classification rates for step 4 model for the pooled sample

	Calibration Sample			Test Sample	
	Male	Female		Male	Female
Male	107/120 89.17%	13/120 10.83%	Male	73/82 89.02%	9/82 10.98
Female	9/120 7.50%	111/120 92.50%	Female	7/60 11.67%	53/60 88.33%
Total Correct	218/240 90.83%		Total Correct	126/142 88.73%	

The fifth and final model included here is a 5-varibale model (Table 17) with an R-squared value of 0.6697 and an F-vaule of 94.89. This model includes the integration of the maximum epiphyseal breadth of the proximal tibia (MEP), the maximum epiphyseal breadth of the distal tibia (MED), the transverse diameter of the tibia at the nutrient foramen (TDN), maximum diameter of the tibia at the midshaft (MDM), and the length from the intercondylar eminence to the nutrient foramen (LIN). One variable, the maximum diameter of the tibia at the midshaft (MDM), exceeds the critical value of <.05, with a partial probability of 0.2099. 90.00% of the males and 90.83% of the females classify correctly within the pooled calibration sample. The overall correct classification rate is 90.42%. When applied to the test sample this model identifies males correctly 87.80% of the time and females 86.67% of the time. The overall correct classification rate is 87.32%.

Table 17. Classification rates for step 5 model for the pooled sample

	Calibration Sample			Test Sample	
	Male	Female		Male	Female
Male	108/120	12/120	Male	72/82	10/82
	90.00%	10.00%		87.80%	12.20%
Female	11/120	109/120	Female	8/60	52/60
	9.17%	90.83%		13.33%	86.67%
Total	217/240		Total	124/142	
Correct	90.42%		Correct	87.32%	

Morphological Variation Among Young Adult Males and Females

The PROC STEPWISE procedure with the MAXR option and the PROC DESCRIM procedure were applied to dimensions of the tibia in the young Black sample. This resulted in

five models, each possessing an associated R-squared value that increases slightly with each successive model (Table 18). An overall model probability of <.0001 exists for each model. Three of the five models also maintain a partial probability of <.05 for each variable. Again, the maximum epiphyseal breadth of the proximal tibia is incorporated in each model. This procedure ceased at five models due to minimal increases in the R-squared value and the inclusion of numerous variables with partial probabilities exceeding the critical value of <.05.

Table 18. Stepwise models for the young adult calibration sample

Step	Variables	R^2	Model F	Partial F	P
1	Maximum epiphyseal breadth of the proximal tibia	0.6878	260.02	260.02	<.0001
2	Maximum epiphyseal breadth of the proximal tibia	0.7055	140.16	53.02	<.0001
	Maximum Epiphyseal breadth of the distal tibia			7.02	0.0092
3	Maximum epiphyseal breadth of the proximal tibia	0.7129	95.99	45.79	<.0001
	Maximum epiphyseal breadth of the distal tibia			6.33	0.0133
	Length from intercondylar eminence to the nutrient foramen			2.96	0.0879
4	Maximum length of the tibia	0.7181	73.25	2.15	0.1448
	Maximum epiphyseal breadth of the proximal tibia			46.14	<.0001
	Maximum epiphyseal breadth of the distal tibia			6.13	0.0147
	Length from intercondylar eminence to the nutrient foramen			5.10	0.0258
5	Maximum length of the tibia	0.7192	73.62	6.87	0.0100
	Maximum epiphyseal breadth of the proximal tibia			84.35	<.0001
	Maximum diameter of the tibia at the nutrient foramen			6.57	0.0116
	Length from intercondylar eminence to the nutrient foramen			11.32	0.0010

All measurements are significant to α=.05

As with the pooled sample, the best single-variable model (Table 19) is represented by the maximum epiphyseal breadth of the proximal tibia (MEP). The R-squared value of 0.6878 and F-value of 260.02 is affiliated with the application of this model on the young Black calibration sample. The correct classification rates for the calibration sample are 96.67% for males and 88.33% for females, with an overall correct classification of 92.50%. Application of the single-variable model on the young adult test sample produced correct classification in

83.33% of the males and 90.32% of the females. Overall, individuals are correctly identified as their respective sex 86.30% of the time.

Table 19. Classification rates for step 1 model for the young adult sample

	Calibration Sample			Test Sample	
	Male	Female		Male	Female
Male	58/60 96.67%	2/60 3.33%	Male	35/42 83.33%	7/42 16.67%
Female	7/60 11.67%	53/60 88.33%	Female	3/31 9.68%	28/31 90.32%
Total Correct	111/120 92.50%		Total Correct	63/73 86.30%	

The second model developed through the stepwise procedure included two variables, the maximum epiphyseal breadth of the proximal tibia (MEP) and the maximum epiphyseal breadth of the distal tibia (MED) (Table 20). The model expresses an R-squared value of 0.7055 and an F-value of 140.16. When applied to the young calibration sample 95.00% of males and 93.33% of females are correctly classified. The overall correct classification is 94.17% in the calibration sample. Sex is correctly identified in the test sample 90.48% of the time for males and 90.32% of the time for females. Overall the test sample produces a correct classification of 90.41% of the specimens.

Table 20. Classification rates for step 2 model for the young adult sample

	Calibration Sample			Test Sample	
	Male	Female		Male	Female
Male	57/60 95.00%	3/60 5.00%	Male	38/42 90.48%	4/42 9.52%
Female	4/60 6.67%	56/60 93.33%	Female	3/31 9.68%	28/31 90.32%
Total Correct	113/120 94.17%		Total Correct	66/73 90.41%	

The third model includes three dimensions, the maximum epiphyseal breadth of the proximal tibia (MEP), maximum epiphyseal breadth of the distal tibia (MED), and the length from the intercondylar eminence to the nutrient foramen (LIN) (Table 21). The model has an associated R-squared value of 0.7129 and an F-vaule of 95.99. Overall, correct classification occurs in 95.00% the young calibration sample. This same value is the correct classification rate for both the sexes of this sample as well. The test sample produces an 88.10% correct classification in males and 93.55% in females. The overall correct classification rate is calculated as 90.41%. One of the variables, the length from the intercondylar eminence to the nutrient foramen (LIN), associated with this model produces a partial probability of 0.0879, therefore surpassing the critical value of <.05.

Table 21. Classification rates for step 3 model for the young adult sample

	Calibration Sample			Test Sample	
	Male	Female		Male	Female
Male	57/60 95.00%	3/60 5.00%	Male	37/42 88.10%	5/42 11.90%
Female	3/60 5.00%	57/60 95.00%	Female	2/31 6.45%	29/31 93.55%
Total Correct	114/120 95.00%		Total Correct	66/73 90.41%	

A four-variable model is utilized in the fourth model (Table 22). It includes the following measurements: the maximum length of the tibia (MLT) the maximum epiphyseal breadth of the proximal tibia (MEP), the maximum epiphyseal breadth of the distal tibia (MED), and the length of the intercondylar eminence to the nutrient foramen (LIN). It produces an R-squared value of 0.7181 and an F-value of 73.25. Both the males and females of the young calibration sample are correctly classified at 96.67%, creating equivalent overall rate. The test sample identifies males correctly in 90.48% of the specimens and 93.55% of the female

specimens. This creates an overall correct classification rate of 91.78% of the young test sample. The partial probability of the maximum length of the tibia (MLT) is 0.1448, which exceeds the critical value of this procedure.

Table 22. Classification rates for step 4 model for the young adult sample

	Calibration Sample			Test Sample	
	Male	Female		Male	Female
Male	58/60 96.67%	2/60 3.33%	Male	38/42 90.48%	4/42 9.52%
Female	2/60 3.33%	58/60 96.67%	Female	2/31 6.45%	29/31 93.55%
Total Correct	116/120 96.67%		Total Correct	67/73 91.78%	

Table 23. Classification rates for step 5 model for the young adult sample

	Calibration Sample			Test Sample	
	Male	Female		Male	Female
Male	59/60 98.33%	1/60 1.67%	Male	39/42 92.86%	3/42 7.14%
Female	1/60 1.67%	59/60 98.33%	Female	2/31 6.45%	29/31 93.55%
Total Correct	118/120 98.33%		Total Correct	68/73 93.15%	

The fifth model incorporates another four variables set, the maximum length of the tibia (MLT) the maximum epiphyseal breadth of the proximal tibia (MEP), the maximum diameter of the tibia at the nutrient foramen (MDN), and the length of the intercondylar eminence to the nutrient foramen (LIN) (Table 23). The R-squared value of 0.7192 demonstrates a slight increase over that associated with the previous four step model, and expresses an F-value of 73.62. Each of the measurements' partial probability falls below the critical value of <.05, consequently creating the optimal four-variable model. The model correctly classifies 98.33% of both males and females, and therefore the producing an overall correct classification of 98.33%

in the young calibration sample. 92.86% of males and 93.55% of females are correctly designated within the young test sample. Correct classification for the entirety of the test sample is 93.15%.

Morphological Variation Among Older Adult Males and Females

The PROC STEPWISE procedure with the MAXR option and PROC DISCRIM procedure was also applied to the older adult Black sample. Five models were produced with R-squared values that decrease slightly over the preceding models (Table 24). Overall, the models exemplify a probability of <.0001. Only the single-variable model and the two-variable model exhibit partial probabilities of <.05, while the other three incorporate one or two variables with partial probabilities that exceed critical value of <.05. The maximum epiphyseal breadth of the proximal tibia (MEP) continues to be utilized in each model developed in the older adult calibration sample. This procedure concludes at five models due to minor increases in the R-square value and the inclusion of numerous variables with partially probabilities exceeding the critical value of <.05.

The best single-variable model once again includes the maximum epiphyseal breadth of the proximal tibia (MEP) (Table 25). The associated R-squared value is 0.6100 and the F-value is 184.55. The older adult sample correctly classifies at 85.00% of males and 93.33% of females, with an overall correct classification of 89.17%. Correct classification of the older adult test sample takes place in 82.50% of all males and 82.76% of all females. This creates an overall correct identification rate of 82.60% for the test sample.

Table 24. Stepwise models for the older adult calibration sample

Step	Variables	R^2	Model F	Partial F	P
1	Maximum epiphyseal breadth of the proximal tibia	0.6100	184.55	184.55	<.0001
2	Length of tibia	0.6270	98.33	5.34	0.0227
	Maximum epiphyseal breadth of the proximal tibia			68.85	<.0001
3	Length of tibia	0.6372	67.92	4.48	0.0364
	Maximum epiphyseal breadth of the proximal tibia			31.13	<.0001
	Maximum diameter of the tibia at the midshaft			3.27	0.0730
4	Length of tibia	0.6439	52.00	3.81	0.0534
	Maximum epiphyseal breadth of the proximal tibia			20.38	<.0001
	Transverse diameter of the tibia at the nutrient foramen			2.17	0.1438
	Maximum diameter of the tibia at the midshaft			3.61	0.0601
5	Maximum length of the tibia	0.6514	42.61	2.45	0.1205
	Length of tibia			3.29	0.0723
	Maximum epiphyseal breadth of the proximal tibia			22.77	<.0001
	Transverse diameter of the tibia at the midshaft			2.62	0.1081
	Maximum diameter of the tibia at the midshaft			3.62	0.0596

All measurements are significant to α=.05

Table 25. Classification rates for step 1 model for the older adult sample

	Calibration Sample			Test Sample	
	Male	Female		Male	Female
Male	51/60	9/60	Male	33/40	7/40
	85.00%	15.00%		82.50%	17.50%
Female	4/60	56/60	Female	5/40	24/40
	6.67%	93.33%		17.24%	82.76%
Total Correct	107/120		Total Correct	57/69	
	89.17%			82.60%	

The second model includes two variables, the length of the tibia (L0T) and the maximum epiphyseal breadth of the proximal tibia (MEP) (Table 26), which produce an associated R-sqaured value of 0.6270 and an F-value of 98.33. Of the specimens in this sample, 85.00% of the males classify correctly, while 91.67% of the females do so. Overall, the older adult calibration sample correctly classifies 88.33% the specimens based on sex. The model correctly

classifies 87.50% of the males and 79.31% of the females in the older adult test sample, with an overall correct classification of 84.06%.

Table 26. Classification rates for step 2 model for the older adult sample

	Calibration Sample			Test Sample	
	Male	Female		Male	Female
Male	51/60 85.00%	9/60 15.00%	Male	35/40 87.50%	5/40 12.50%
Female	5/60 8.33%	55/60 91.67%	Female	6/29 20.69%	23/29 79.31%
Total Correct	106/120 88.33%		Total Correct	58/69 84.06%	

Three measurements of the tibia are used to develop the third model (Table 27). These measurements include the length of the tibia (L0T), the maximum epiphyseal breadth of the proximal tibia (MEP), and the maximum diameter of the tibia at the midshaft (MDM). The R-squared value of this model is 0.6372 and the F-value is 67.92. Of the measurements within this model, partial probability of the maximum diameter of the tibia at the midshaft (MDM) exceeds the critical value of <.05, while the other partial probabilities remain statistically significant. When applied to the older adult calibration sample, this model correctly identifies 86.67% of males and 93.33% of females, which produces a 90.00% correct classification rate for the entire calibration sample. Within the test sample, correct classification occurs in 90.00% of the males and 82.76% of the females. This results in an overall correct classification of 86.96%.

Table 27. Classification rates for step 3 model for the older adult sample

	Calibration Sample			Test Sample	
	Male	Female		Male	Female
Male	52/60 86.67%	8/60 13.33%	Male	36/40 90.00%	4/40 10.00%
Female	4/60 6.67%	56/60 93.33%	Female	5/29 17.24%	24/29 82.76%
Total Correct	108/120 90.00%		Total Correct	60/69 86.96%	

The fourth model combines four variables (Table 28), the length of the tibia (L0T), the maximum epiphyseal breadth of the proximal tibia (MEP), the tranverse diameter of the tibia at the nutrient foramen (TDN), and the maximum diameter of the tibia at the midshaft (MDM), to produce an R-squared value of 0.6439 and an F-value of 52.00. Applying this model to the older adult sample correctly classifies 88.33% of males and 93.33% of females, creating an overall correct classification rate of 90.83%. Correct classification occurs in 87.50% of males and 82.76% of females when this model is applied to the older adult test sample. An 85.51% correct classification is associated with the overall sample. The partial probability associated with the transverse diameter of the tibia at the midshaft (TDM) surpasses the critical value of <.05, while the other measurements exhibit partial probabilities of < .05.

Table 28. Classification rates for step 4 model for the older adult sample

	Calibration Sample			Test Sample	
	Male	Female		Male	Female
Male	53/60 88.33%	7/60 11.67%	Male	35/40 87.50%	5/40 12.50%
Female	4/60 6.67%	56/60 93.33%	Female	5/29 17.24%	24/29 82.76%
Total Correct	109/120 90.83%		Total Correct	59/69 85.51%	

The final model developed is a five-variable model which includes the maximum length of the tibia (MLT), the length of the tibia (L0T), the maximum epiphyseal breadth of the proximal tibia (MEP), the transverse diameter of the tibia at the nutrient foramen (TDN) and the maximum diameter of the tibia at the midshaft (MDM) (Table 29). An R-squared value of 0.6514 and an F-value of 42.61 is expressed by this five-variable model. This model creates classification rates of 88.33% in the males and 91.67% in the females among the specimens of

the older adult calibration sample. This produces an overall correct classification rate of 90.00%. The specimens of the test sample are correctly identified as their respective sexes in 87.50% of the males and 82.76% of the females, producing an overall correct classification rate of 85.51%. Four of the measurements exemplify partial probabilities greater than or equal to .05. Only the maximum epiphyseal breadth of the proximal tibia (MEP) retains a partial probability of < .05.

Table 29. Classification rates for step 5 model for the older adult sample

	Calibration Sample			Test Sample	
	Male	Female		Male	Female
Male	53/60 88.33%	7/60 11.67%	Male	35/40 87.50%	5/40 12.50%
Female	5/60 8.33%	55/60 91.67%	Female	5/29 17.24%	24/29 82.76%
Total Correct	108/120 90.00%		Total Correct	59/69 85.51%	

The Interaction of Stature and Tibial Morphology

The correlation between cadaver height and the tibial dimensions collected during this study were assessed through the application of the PROC REG procedure. The models developed were each significant at <.05. This multivariate statistic was applied to multiple calibration samples (pooled, female, male, young adult female, young adult male, older adult female, and older adult male) to evaluate the degree by which variables reflect the stature of an individual. For the purposes of this study, the three models with the highest R-squared values will be discussed, in addition to the model exemplifying the lowest R-squared value. Every model is presented in Tables 30 through 36 in respect to its appropriate calibration sample.

Each model produced from the tibial measurements within the pooled calibration sample are significant at <.0001 (Table 30). The maximum length of the tibia (MLT) provides the

highest explanation of the dependent variable with an R-squared of 0.7147. The next highest R-squared value of 0.7072 is expressed by the length of the tibia (L0T), which is slightly lower at than the preceding dimension. The maximum epiphyseal breadth of the proximal tibia (MEP) represents the next best R-squared value of 0.5551. The lowest R-squared value (0.2660) is demonstrated by the transverse diameter of the tibia at the nutrient foramen (TDN).

Table 30. Linear regression models for the pooled calibration sample

Variables	**R^2**	**Model F**	**P**
Maximum length of the tibia	0.7147	596.16	<.0001
Length of the tibia	0.7072	574.76	<.0001
Maximum epiphyseal breadth of the proximal tibia	0.5551	296.98	<.0001
Maximum epiphyseal breadth of the distal tibia	0.4423	188.77	<.0001
Anterior/Posterior epiphyseal breadth of the distal tibia	0.4438	189.91	<.0001
Maximum diameter of the tibia at the nutrient foramen	0.4104	165.64	<.0001
Transverse diameter of the tibia at the nutrient foramen	0.3175	110.74	<.0001
Maximum diameter of the tibia at the midshaft	0.3991	158.05	<.0001
Transverse diameter of the tibia at the midshaft	0.2660	86.24	<.0001
Length from intercondylar eminence to the nutrient foramen	0.3077	105.80	<.0001
Circumference of the tibia at the nutrient foramen	0.5019	239.83	<.0001
Circumference of the tibia at the midshaft	0.4027	160.46	<.0001

Values are significant at $\alpha < .05$

This procedure was then preformed on the female calibration sample, where the R-squared values are reduced for each of the dimensions in comparison to the pooled sample (Table 31). The dimensions each express significance at <.05. The maximum length of the tibia (MLT) again demonstrates the highest R-squared value in this sample at 0.5163, followed by the length of the tibia (L0T) with an R-squared value of 0.5003. The next highest R-squared value is reduced to 0.2941 and is represented by the circumference of the tibia at the nutrient foramen (C0N). The measurement that expresses the poorest R-squared value is the maximum diameter of the tibia at the midshaft (MDM), which is 0.0849.

Table 31. Linear regression models for the female calibration sample

Variables	R^2	Model F	P
Maximum length of the tibia	0.5163	125.97	<.0001
Length of the tibia	0.5003	118.14	<.0001
Maximum epiphyseal breadth of the proximal tibia	0.1979	29.12	<.0001
Maximum epiphyseal breadth of the distal tibia	0.2464	38.58	<.0001
Anterior/Posterior epiphyseal breadth of the distal tibia	0.2027	30.00	<.0001
Maximum diameter of the tibia at the nutrient foramen	0.1633	23.03	<.0001
Transverse diameter of the tibia at the nutrient foramen	0.1600	22.48	<.0001
Maximum diameter of the tibia at the midshaft	0.0849	10.95	0.0012
Transverse diameter of the tibia at the midshaft	0.1424	19.60	<.0001
Length from intercondylar eminence to the nutrient foramen	0.1619	22.80	<.0001
Circumference of the tibia at the nutrient foramen	0.2941	49.16	<.0001
Circumference of the tibia at the midshaft	0.2045	30.33	<.0001

Values are significant at $\alpha < .05$

Table 32. Linear regression models for the male calibration sample

Variables	R^2	Model F	P
Maximum length of the tibia	0.6385	208.40	<.0001
Length of the tibia	0.6309	201.73	<.0001
Maximum epiphyseal breadth of the proximal tibia	0.4063	80.75	<.0001
Maximum epiphyseal breadth of the distal tibia	0.1310	17.80	<.0001
Anterior/Posterior epiphyseal breadth of the distal tibia	0.1845	26.69	<.0001
Maximum diameter of the tibia at the nutrient foramen	0.1994	29.38	<.0001
Transverse diameter of the tibia at the nutrient foramen	0.0883	11.43	0.0010
Maximum diameter of the tibia at the midshaft	0.2454	38.38	<.0001
Transverse diameter of the tibia at the midshaft	0.0800	10.26	0.0017
Length from intercondylar eminence to the nutrient foramen	0.1677	23.78	<.0001
Circumference of the tibia at the nutrient foramen	0.2403	37.33	<.0001
Circumference of the tibia at the midshaft	0.1361	18.59	<.0001

Values are significant at $\alpha < .05$

The male calibration sample follows a trend similar to the pooled sample, where the same three dimensions possess the strongest relationship with stature (Table 32). These include the maximum length of the tibia (MLT), the length of the tibia (L0T), and the maximum epiphyseal breadth of the proximal tibia (MEP). Their R-squared values are 0.6385, 0.6309, and 0.4063, respectively. The transverse diameter of the tibia at the midshaft (TDM) demonstrates the lowest R-squared value of this sample at 0.0800, but is followed very closely by the transverse diameter

of the tibia at the nutrient foramen (TDN), which is characterized by an R-squared value of 0.0883. Each of the models are again significant at <.05.

When applied to the young adult female calibration sample each of the models remain significant at <.05 (Table 33). The maximum length of the tibia (MLT) posses the strongest R-squared value associated with this sample at 0.5545. The next highest R-squared value is 0.5408, which is represented by the length of the tibia (L0T). This measurement is followed by the circumference of the tibia at the midshaft (C0M) in reference to its R-squared value of 0.4031. The weakest R-squared value affiliated with this sample is 0.0777 which is represented by the length from the intercondylar eminence to the nutrient foramen (LIN).

Table 33. Linear regression models for the young adult female calibration sample

Variables	**R^2**	**Model F**	**P**
Maximum length of the tibia	0.5545	72.19	<.0001
Length of the tibia	0.5408	68.29	<.0001
Maximum epiphyseal breadth of the proximal tibia	0.2894	23.62	<.0001
Maximum epiphyseal breadth of the distal tibia	0.3299	28.56	<.0001
Anterior/Posterior epiphyseal breadth of the distal tibia	0.3321	28.85	<.0001
Maximum diameter of the tibia at the nutrient foramen	0.2985	24.68	<.0001
Transverse diameter of the tibia at the nutrient foramen	0.1784	12.59	0.0008
Maximum diameter of the tibia at the midshaft	0.2890	23.58	<.0001
Transverse diameter of the tibia at the midshaft	0.1467	9.97	0.0025
Length from intercondylar eminence to the nutrient foramen	0.0777	4.89	0.0310
Circumference of the tibia at the nutrient foramen	0.3543	31.83	<.0001
Circumference of the tibia at the midshaft	0.4031	39.17	<.0001

Values are significant at $\alpha < .05$

The maximum length of the tibia (MLT) holds the best R-squared value of 0.5809 in the young adult male calibration sample (Table 34). This is followed by the length of the tibia (L0T) with an R-squared of 0.5703. The next highest value of 0.3240 is represented by the maximum epiphyseal breadth of the tibia (MEP). The transverse diameter of the tibia at the midshaft (TDM) is associated with the lowest R-squared value of 0.0473, which also possesses the only insignificant probability associated with this sample.

Table 34. Linear regression analysis for the young adult male calibration sample

Variables	R^2	Model F	P
Maximum length of the tibia	0.5809	80.38	<.0001
Length of the tibia	0.5703	76.97	<.0001
Maximum epiphyseal breadth of the proximal tibia	0.3240	27.80	<.0001
Maximum epiphyseal breadth of the distal tibia	0.0960	6.16	0.0160
Anterior/Posterior epiphyseal breadth of the distal tibia	0.1599	11.04	0.0016
Maximum diameter of the tibia at the nutrient foramen	0.1182	7.78	0.0072
Transverse diameter of the tibia at the nutrient foramen	0.0672	4.18	0.0454
Maximum diameter of the tibia at the midshaft	0.1865	13.30	0.0006
Transverse diameter of the tibia at the midshaft	0.0473	2.88	0.0950
Length from intercondylar eminence to the nutrient foramen	0.2515	19.49	<.0001
Circumference of the tibia at the nutria nt foramen	0.1550	10.64	0.0019
Circumference of the tibia at the midshaft	0.1675	11.67	0.0012

Values are significant at $\alpha < .05$

Table 35. Linear regression analysis for the older adult female calibration sample

Variables	R^2	Model F	P
Maximum length of the tibia	0.4729	52.03	<.0001
Length of the tibia	0.4568	48.78	<.0001
Maximum epiphyseal breadth of the proximal tibia	0.1638	11.36	0.0013
Maximum epiphyseal breadth of the distal tibia	0.2153	15.91	0.0002
Anterior/Posterior epiphyseal breadth of the distal tibia	0.1368	9.19	0.0036
Maximum diameter of the tibia at the nutrient foramen	0.0728	4.55	0.0371
Transverse diameter of the tibia at the nutrient foramen	0.1258	8.35	0.0054
Maximum diameter of the tibia at the midshaft	0.0069	0.40	0.5281
Transverse diameter of the tibia at the midshaft	0.1732	12.15	0.0009
Length from intercondylar eminence to the nutrient foramen	0.2916	23.88	<.0001
Circumference of the tibia at the nutrient foramen	0.2434	18.66	<.0001
Circumference of the tibia at the midshaft	0.1006	6.49	0.0136

Values are significant at $\alpha < .05$

When applied to the older adult female calibration sample, the linear regression procedure produces the highest R-squared values among the maximum length of the tibia (MLT) and the length of the tibia (L0T) with the respective values of 0.4729 and 0.4568 (Table 35). The length from the intercondylar eminence to the nutrient foramen (LIN) demonstrates the next highest R-squared value of 0.2916. The lowest R-squared value is 0.0069 and is represented by

the maximum diameter of the tibia at the midshaft (MDM), which also displays the only insignificant probability within this sample.

Within the older adult male calibration sample the highest R-squared value of 0.6917 is achieved by the maximum length of the tibia (MLT) (Table 36). This is followed by the length of the tibia (L0T) which is affiliated with an R-squared value of 0.6811. The next highest R-squared value of 0.4641 is demonstrated by the maximum epiphyseal breadth of the proximal tibia (MEP). Of the dimensions, the lowest R-squared value is 0.1040 which is affiliated with the transverse diameter of the tibia at the nutrient foramen (TDN). Each of these models are represented by significant probabilities.

Table 36. Linear regression models for the older adult male calibration sample

Variables	**R^2**	**Model F**	**P**
Maximum length of the tibia	0.6917	130.11	<.0001
Length of the tibia	0.6811	123.88	<.0001
Maximum epiphyseal breadth of the proximal tibia	0.4641	50.24	<.0001
Maximum epiphyseal breadth of the distal tibia	0.1615	11.17	0.0015
Anterior/Posterior epiphyseal breadth of the distal tibia	0.2000	14.50	0.0003
Maximum diameter of the tibia at the nutrient foramen	0.2568	20.04	<.0001
Transverse diameter of the tibia at the nutrient foramen	0.1040	6.73	0.0120
Maximum diameter of the tibia at the midshaft	0.3086	25.89	<.0001
Transverse diameter of the tibia at the midshaft	0.1171	7.69	0.0074
Length from intercondylar eminence to the nutrient foramen	0.1250	8.28	0.0056
Circumference of the tibia at the nutrient foramen	0.3022	25.12	<.0001
Circumference of the tibia at the midshaft	0.1256	8.33	0.0055

Values are significant at $\alpha < .05$

CHAPTER FIVE

DISCUSSION

Size and Shape Variation of the Tibia

This study explores the size and shape variation of the human tibia that is represented by traditional and non-traditional measurements through the application of univariate and multivariate statistics. The PROC CORR procedure revealed the way in which the morphology of the tibia varies; specifically, how the tibial dimensions covary among one another. The means of each of the dimensions attest to the sexual dimorphic nature of the tibia throughout adult life, while the distributions of the scores reveal great variation exists within the sexes. The variations due to the natural aging process of the human body are highlighted by the summary statistics as well. The combination of the PROC STEPWISE and PROC DISCRIM procedures allowed for the assessment of the manner by which the measurements account for the morphological variation of the tibia among and between males and females, while also evaluating the accuracy of these variables to do so. Finally, the PROC REG procedure was utilized to assess the capability of the tibial dimensions to explain the stature variation within the sample.

Covariance of Tibial Dimensions

Utilizing the PROC CORR procedure enabled the evaluation of the relationships that exist in the size and shape variation expressed by human tibiae (Tables 5-11). This statistic addresses the degree to which two variables correlate, in this case the tibial dimensions, as well as the directionality of the relationships. Strong positive correlations are expressed between multiple dimensions of the tibia, especially those that are variations of the same measurement (e.g. the maximum length of the tibia [MLT] and the length of the tibia [L0T]). Variability within the dimensions is also represented by the weak

relationships, such as those associations with the length from the intercondylar eminence to the nutrient foramen (LIN).

The most consistent and obvious relationships are depicted by those measurements that are variations of the same dimension or those quantifying the same features of the tibia. The strongest correlation in every sample is represented by the relationship between the maximum length of the tibia (MLT) and the length of the tibia (L0T). In each case these dimensions express a nearly perfect, positive correlation, meaning as one dimension enlarges, a corresponding increase is seen in the other. This pattern is also exemplified when one of these dimensions decreases in size.

The same is true for those dimensions taken at the level of the nutrient foramen and the midshaft. Quantification at the level of the nutrient foramen, no matter the orientation of the measurement, produces consistently high positive correlations between dimensions taken at this location. While the measurements at the midshaft do covary, this relationship is sporadically expressed across the samples. This suggests that while the diaphysis appears to increase and decrease in size proportionally, this positive correlation is more precisely represented on the proximal end of the tibial shaft, at the location of the nutrient foramen. In other words, the shape of the midshaft varies more than that of the diaphysis at the level of the nutrient foramen.

Covariance is also displayed between the measurements of the diaphysis. Primarily, this is represented by the relationship between the circumference of the nutrient foramen (C0N) and the maximum diameter of the midshaft (MDM), in that each sample demonstrates a positive correlation between these two dimensions. This further supports the suggestion that the shape of the shaft of the tibia expresses a positive covariance, meaning that an increase or decrease in shape is typically reflected by the tibial shaft as a whole.

Strong positive correlations are represented between the dimensions of the proximal end and the distal end (the maximum epiphyseal breadth of the proximal tibia [MEP], the maximum epiphyseal breadth of the distal tibia [MED], the anterior/posterior epiphyseal breadth of the distal tibia [AED]) in the pooled calibration sample. These correlations are not well represented by the remaining samples. The

female calibration samples, including that of the young adult and older adult samples, expressed moderate correlations between these dimensions. Conversely, the male calibration sample demonstrates minimal to no correlations between the measurements taken at the ends of the diaphysis. This suggests that variation in the manner by which the tibia covaries at the proximal and distal ends differs between the sexes. The disparities observed between the sexes is more likely due to secular effects in the female sample, rather than sexual dimorphism.

The maximum epiphyseal breadth of the proximal tibia (MEP) consistently provides moderate to strong correlations with the maximum length of the tibia (MLT) in each of the calibration samples. It is evident that the articular breadth of the proximal end of the tibia enlarges as the length of the tibia expands. This relationship should be assessed in further detail to completely understand the covariance of the two dimensions, as well as to determine if sex and age effects that were not represented by this sample impact the correlation.

Throughout the entirety of the sample the length from the intercondylar eminence to the nutrient foramen (LIN) exhibits minimal to no correlation with the other dimensions collected during this study. The only exception is demonstrated by the relationship between this measurement and the length of the tibia (L0T), as well as, the maximum length of the tibia (MLT), where moderate positive correlations exist. The correlation coefficients associated with these two relationships ranges from 0.4638 to 0.6400. This indicates that the length from the intercondylar eminence to the nutrient foramen (LIN) is a highly variable dimension. The only correlations that exist are between the other linear dimensions of the bone, which are minimal in the majority of the samples. This supports previous research which declares that the location of the nutrient foramen is highly variable within the upper one-third of the tibia diaphysis (Kizilkanat et al., 2007). The correlation with the length of this long bone implies that, although minor, there may be positive correlation between the location of the nutrient foramen and the total length of the tibia. This relationship should be explored in further detail in order to better comprehend the way the nutrient foramen varies in relation to the tibia as a whole, as well as other aspects of the tibia.

Morphological Variation Within and Between the Sexes

The univariate and multivariate statistics applied to the tibial dimensions clearly illustrate the sexually dimorphic nature of the human species. In particular, the descriptive statistics highlight the fact that males are generally larger and more robust than females (Table 2-4). The mean for each of the twelve dimensions is consistently larger among the males than the females. This trend transcends the aging processes to remain true throughout life. The largest discrepancies between the sexes is expressed by the linear dimensions, the maximum length of the tibia (MLT), the length of the tibia (L0T), and the length from the intercondylar eminence to the nutrient foramen (LIN), demonstrating the size variation between the sexes that is represented by the tibial dimensions. This trend is reflective of living height, a sexually dimorphic trait, which is well documented as possessing a direct relationship with long bone length (Trotter and Glesser, 1952; 1958; Steele, 1970; Steele and McKern, 1969; Meadows and Jantz, 1995; Jantz and Jantz, 1999). The means associated with the circumference of the tibia at the nutrient foramen (C0N) and the circumference of the tibia at the midshaft (C0M) are separated by approximately 10 millimeters, demonstrating the shape variation of the tibia between the sexes. These dimensions suggest that the diaphysis of the tibia is more robust among males than among females. Alternatively, the means of the transverse diameter of the tibia at the nutrient foramen (TDN) and the transverse diameter of the tibia at the midshaft (TDM) exhibit the smallest degree of difference between the sexes. Either the transverse dimensions poorly represent the shape variation of the tibia or the diaphysis of the tibia expresses minimal sexual dimorphism when quantified transversely.

The linear dimensions also represent the greatest distribution of the mean values across males and females. This indicates that variation not only exists between the sexes, but is also evident among them. Each of the dimensions are characterized by this trend in varying degrees. This creates overlap of the values between the sexes, further demonstrating the range of variation that exists within them. This

demonstrates that while quantification of the tibia is representative of the size and shape variation between males and females, it is not a finite descriptor of sex.

The PROC STEPWISE procedure with a MAXR option, followed by the PROC DISCRIM procedure were employed to further assess the variability demonstrated by the summary statistics, while also assessing the capacity of the variables to discriminate sex from this variability (Table 12-17). The first five models produced through the application of the stepwise procedure were discussed, but are not all necessarily recommended. The stepwise procedure functions to determine the best predictors of sex and then develops models based on the measurements' abilities to account for the variability expressed by the sexes. The models begin with the best single-variable predictor and progress by adding an additional variable with each step in order to maximize the model's associated R-squared value. In some cases multiple models with the same number of variables are developed in order to maximize the classification potential of the model.

Application of the stepwise procedure to the pooled sample produces five models that, with each additional variable, express a slight increase in the R-squared value. The second model utilizes the maximum epiphyseal breadth of the distal tibia (MED) in addition to the best single-variable. Although the R-squared value increases with this model, correct classification decreases among the males of the calibration sample to 88.33%, but increases marginally in the females to 90.83%. The third model includes those tibial measurements of the second model, as well as the length from the intercondylar eminence to the nutrient foramen (LIN). Correct estimation of sex in males remains at 88.33% and increases once again within the female calibration sample, reaching 92.50%. Step four produces a four-variable model that includes the maximum epiphyseal breadth of the proximal tibia (MEP), the maximum epiphyseal breadth of the distal tibia (MED), the transverse diameter of the tibia at the midshaft (TDM) and the length from the intercondylar eminence to the nutrient foramen (LIN). This model correctly classifies 89.02% of the males and 88.33% of the females in the calibration sample. The fifth model expresses a slight increase in the R-squared value, as well as the classification rates among both sexes.

Unfortunately, the fifth model is not recommended due to the inclusion two variables with an associated insignificant partial probability.

Slight reductions are displayed when each model is applied to the test sample, but accuracy is consistently high. The single-variable model proves to be a good indicator of sex in the pooled sample, where accurate classification occurs in 85.37% of males and 86.67% of females among the pooled test sample. The second model is slightly more successful in both sexes, males being correctly classified 87.80% and 86.67% of females. The third model developed increases the accuracy of predicting sex in men to 87.80% over the preceding step. Accuracy in women, on the other hand, is reduced to 83.67%. The fourth model correctly identifies 89.02% of the males and 88.33% of the females. Throughout the application of these models to the pooled and test samples, females classify with slightly less accuracy than males.

The consistent inclusion of the maximum epiphyseal breadth of the proximal tibia (MEP) suggests that the proximal end may represent the most sexually distinct variation of the tibia. This supports conclusions made by Holland (1991) concerning the proximal end of the tibia. His study included a sample of white and black individuals from the Hamann-Todd Osteological Collection, which involved the quantification of the proximal end of the tibia. Of the measurements he evaluated, the "biarticular breadth," a variation of the maximum epiphyseal breadth of the proximal tibia (MEP), best distinguished sex in 95.00% of his sample. His results are slightly higher than those associated with this study's overall correct classification of the pooled sample from the best single-variable predictor. Within the calibration sample, 91.66% of the individuals were correctly identified, while 85.92% of the test sample was correctly classified. The higher accuracy resulting from Holland's (1991) study could result for numerous reasons. Primarily, the manner in which the measurement is taken is slightly different. The study at hand utilized the osteometric board when measuring this aspect. Holland (1991) used sliding calipers. Also, the samples utilized are characterized by different parameters. Holland's sample consisted of two group affiliations and a small sample size of 100 individuals, where secular variation and age related changes were not accounted for. Despite these inconsistencies between the studies, both

conclude that, when quantified, the breadth of the articular surface of the proximal end of the tibia provides a highly accurate method of evaluating sexual variation.

The Effects of Age on the Morphology of the Tibia

The same methods of analyses discussed above were also applied to the young adult and older adult calibration and test samples (Table 18-29). The summary statistics for these samples illustrate the morphological variation between the two age groups. The stepwise procedures produce models that vary slightly in the young adult sample compared to those formulated from the pooled sample. Those of the older adult sample are considerably different from either of the previous two samples utilized in the same evaluation, suggesting the morphology of the tibia is altered to some degree with increasing age. Classification rates are derived for both the calibration samples and the test samples, demonstrating the accuracy of the models to correctly identify sex with the progression of age.

On average, the summary statistics demonstrate an enlargement of tibial dimensions as age increases. Nine of the twelve measurements in males and seven in females increase from the young adult samples to the older adult samples. This pattern is consistent with the normal aging process, where osteoarthritis impacts the majority of older individuals through the accumulation of osteophytic lipping, thereby altering the size and shape of the tibia (Loeser, 2010; Loeser and Shakoor, 2003). Unlike the males, the overall length of the tibia, as demonstrated by the means of the maximum length of the tibia (MLT) and the length of the tibia (L0T), decreases from the young adult female sample to older adult female sample. While this may be related to degenerative differences between the sexes, it also may be the result of temporal variation, as the female sample was unable to be restricted by birth year.

In the case of the young adult calibration sample, five models were produced through the stepwise procedure that best discriminate sex within the sample (Table 18-23). The first three steps follow the same pattern associated with the pooled sample of progressively adding a variable to each step in order to produce the best R-squared value. The fourth and fifth steps both produce four-variable models, where the fourth step possesses a lower R-squared and includes a insignificant partial probability.

Therefore, step five represents the best four-variable model in the young adult calibration. When classified, both the calibration samples and test samples produce accurate results.

The best single-variable model is the maximum epiphyseal breadth of the proximal tibia (MEP), which is again utilized in every model developed from the young adult calibration sample. Males are correctly distinguished 96.67% of the time, while females are 88.33% of the time. The second model involves the maximum epiphyseal breadth of the proximal tibia (MEP), as well as the maximum epiphyseal breadth of the distal tibia (MED), which generates correct classification rates of 95.00% in males and 93.33% in females. While the third and fourth models identify sex of an individual with high accuracy, it is suggested that they be disregarded due to insignificant partial probabilities associated with individual variables utilized by the models in order to avoid the increased probability of incorrectly identifying sex. The fifth model incorporates four measurements which includes the following: the maximum length of the tibia (MLT), the maximum epiphyseal breadth of the proximal tibia (MEP), the maximum diameter of the tibia at the nutrient foramen (MDN) and the length from the intercondylar eminence to the nutrient foramen (LIN). This model is the best four-variable model produced through this calibration sample due to the R-squared value of 0.7192 and the inclusion of variables that express significant partial probabilities. Classification results consist of 92.86% of males and 93.55% of females being correctly identified.

When these models are tested on the independent young adult test sample accurate classification results are produced in varying percentages. The best single-variable model indicates the sex of males correctly in 83.33% of the test sample and females in 90.32% of the test sample, creating an overall classification of 86.30%. The second model produces slightly higher classification results in males (90.48%) and remains the same in females (90.32%). This increases the overall classification of the young adult test sample by approximately 4.00%, with a final correct classification rate of 90.41%. Lastly, the fifth model produces the highest overall rate of 93.15%, where 92.86% of males are correctly identified and 93.55% of females are correctly classified. Based on these rates, it is recommended that the fifth model developed through this procedure be utilized if the age at death is known to fall into the

young adult age group and if complete tibiae are present because correct identification in both males and females occurs with the highest accuracy in this model.

The continued presence of the maximum epiphyseal breadth of the proximal tibia (MEP) in the models developed from the young adult sample further supports the conclusion that quantification of the proximal end best represents the morphological discrepancies between the sexes in the young adult sample, as well as the pooled sample. Each of the models produced from the young adult sample maintain higher R-squared values than those associated with the pooled sample. The first three models are identical for both samples. The higher R-squared values affiliated with the young adult sample suggests that less variation exists within the sexes in the young adult sample when compared to the pooled sample, therefore allowing the independent variables to better account for the variability of the dependent variable (sex). This is also represented by the correct classification rates of these two models, where accuracy is higher in the young adult test sample than the pooled test sample.

The models produced from the older adult calibration sample vary greatly from those of the previous two samples discussed (Table 24-29). The incorporation of the maximum epiphyseal breadth of the proximal tibia (MEP) persists in the older adult models. As the single-variable model, this measurement correctly evaluates sex in the calibration sample in 85.00% of the males and 93.33% of the females. The second step in the procedure adds the length of the tibia (L0T) to the model. Classification remains at 85.00% for the males and decreases slightly among the females to 91.67%. Unfortunately, only the first two models are recommended due to partial probabilities affiliated with the third, fourth, and fifth models that exceed the significance level of <.05. Higher partial probability suggests that misclassification may occur more often within this sample, likely due to higher morphological variation exhibited by the older adult specimens.

The accuracy of the first and second models decreases when applied to the test sample, but again, efficiently classify males and females. The maximum epiphyseal breadth of the proximal tibia (MEP) allows for 82.50% of the males to be correctly identified, while 82.76% of the females are correctly

identified. In the second model correct classification increases in males to 87.50%, but decrease in the females to 79.31%,the lowest classification rate associated with this study.

Despite any morphological variations that may occur between the age groups, the maximum epiphyseal breadth of the proximal tibia (MEP) is consistently the best single-variable indicator of sex among these samples. Consequently, it is recommended that this measurement be used when the age of a specimen is unknown, as well as under circumstances where age is known and limitations require you to use only the proximal end of the tibia. This contrasts with the results of a previous study on a Black and White sample from the Robert J. Terry Anatomical Skeletal Collection, which stipulates that the circumference of long bones provide the most accurate evaluation of the morphological variation between the sexes (İşcan and Miller-Shaivitz, 1984). The stepwise procedures did not incorporate any of the circumference measurements into the models produced, signifying that these dimensions did not adequately account for the variation associated with the sex of an individual in this study.

Although each model is not suggested for application, the inclusion of the length of the tibia (L0T) in four out of the five models is unique to the older adult calibration sample and therefore deserves to be noted. The most apparent conclusion is that when applied to the older adult calibration sample the dimensions vary from those of the pooled and young adult sample, an observation which is supported by the summary statistics. Further, the summary statistics illustrate that, overall, the aging processes affects males and females by increasing the size and shape of the tibia that is represented by the dimensions. The reliance on the length of the tibia (L0T) to aid in the determination of sex in the older adult sample indicates that variation between the sexes that occurs with increasing age is most consistent at this dimension.

The Interaction of Stature and Tibial Morphology

To investigate the relationship of the tibial morphology and stature, the tibial dimensions are compared to cadaver height through the application of the PROC REG procedure. The relationship of

each measurement was assessed individually within its affiliated calibration samples in order to discern which best represents the variability of that expressed by cadaver height, concurrently identifying the best predictor variable of stature. The calibration samples selected for this procedure allow the impact of the variability expressed among and between the sexes, as well as their respective age groups to be assessed.

Throughout the calibration samples trends can be discerned in respect to the ability of areas or features of the tibia being quantified to explain the variation in stature (Tables 30-36). As was expected, the linear dimensions of the maximum length of the tibia (MLT) and the length of the tibia (L0T) consistently express the highest R-squared values, respectively, for each of the calibration samples. The positive correlation between long bone length and stature has been extensively documented over the last century, and this study provides further support for such conclusions (Muller, 1935; Trotter and Glesser 1952; 1958; Steele, 1970; Steele, 1970; Meadows and Jantz, 1995; Jantz and Jantz, 1999). Conversely, the dimensions of the diaphysis continuously produce lower R-squared values, suggesting that these dimensions provide less adequate predictions of stature in the calibration samples. Although minimally, the diaphysis tends to explain the variability associated with female stature slightly better than that of the males. This is not the case for the older adult female calibration sample, where the R-squared values associated with the diaphyseal measurements is on average lower than the older adult male calibration sample. Overall, the R-squared values associated with the diaphyseal dimensions remain too low to suggest the models be utilized for stature prediction. These low values indicate that when quantified, the shape of the diaphysis, regardless of sex and age, does not explain the variation within the cadaver heights of the samples as efficiently as the total length of the bone. Therefore, as stature fluctuates, a concordant pattern in the manner by which the shape of the diaphysis changes could not be discerned.

Patterns were also indentified in relation to the dimensions of the proximal and distal ends of the tibia. In most samples, the proximal end achieves the highest R-squared value, next to those dimensions associated with tibial length. The exceptions are only present within the female samples where the R-squared value affiliated with the maximum epiphyseal breadth of the tibia at the proximal end (MEP) demonstrates that there is nearly no explanation of the statures of the sample by this variable.

Contrastingly, this dimension represents a moderate amount of the stature variation expressed within the pooled sample and each of the male samples, and in each case is the next best predictor of stature, following the maximum length of the tibia (MLT) and the length of the tibia (L0T). Neither measurement of the distal end of the tibia accounts for much of the stature variation represented in the samples. The highest R-squared value produced for the maximum epiphyseal breadth of the distal tibia (MED) and the anterior/posterior epiphyseal breadth of the tibia (AEP) is associated with the pooled sample, but is low for the remaining samples. This either suggests the way the shape of the distal end varies does not do so in relation to stature or that these dimensions were unable to capture the variation accordingly.

When the models are evaluated in respect to increasing age, variation between the sexes is clearly demonstrated by the R-squared values. The ability of nine of the twelve measurements to explain the stature variation within the female samples decreases as age increases. This suggests that the alteration of tibial morphology with progressing age is impeding the ability of the dimensions to appropriately predict stature. An opposing trend is depicted between the young adult males and the older adult males. The majority of the R-squared values associated with the male samples increases as age increases. Unlike the females, this suggests that the changes in morphology associated with age in the males more efficiently explains stature than the morphology of preceding years. However, it must be kept in mind the potential impact of secular variation. Temporal variation is likely to be expressed to a greater degree within the female sample due to the inclusion of all available birth years in the older adult female sample, while the older adult male sample was restricted to a twelve year birth range. Therefore, the variation expressed between the way in which age affects the variables as predictors of stature may be the result of changes in morphology, as well as stature over time.

The Assessment of Human Variation from Traditional and Non-Traditional Measurements

The majority of methods employed in the assessment of human variation from skeletal remains requires complete, undamaged skeletal elements for accurate and precise application. Ten of the twelve measurements utilized in this study quantify features or areas of the tibia, opposed to the total length of

the bone. The ability of the measurements to represent the morphological variation present within the sample is discussed in order to address the need for alternative techniques of quantifying skeletal elements in forensic and archaeological settings.

The PROC CORR procedure identified the covariance represented by multiple measurements of the tibia, especially those that are variations of the same dimensions. This suggests that the quantification of locations such as the nutrient foramen and the midshaft produce similar results, enabling them to be used as alternatives to one another should damage conflict with one of the dimensions. Although, further research is needed, the correlations represented between the diaphyseal dimensions at the level of the nutrient foramen and midshaft suggest that measurements at these locations are interchangeable when quantifying the diaphysis of the tibia. A relationship between the articular breadth of the proximal tibia and the total length of the bone was also identified in this procedure, suggesting that in cases where total length is not obtainable, the maximum epiphyseal breadth of the proximal tibia (MEP) offers a valid alternative so long as the relationships between the dimensions is fully understood. Alternatives such the ones described here would help ensure the proper analyses of fragmentary remains.

Multiple measurements involving the quantification of features or areas of the tibia also proved useful when reconstructing the sex or stature of a specimen. In respect to the discrimination of sex, the maximum epiphyseal breadth of the proximal tibia (MEP) is continuously the best single-variable model in each sample, regardless of age and sex. It is also included in numerous multi-variable models, aiding in the accurate identification of sex. Overall, the sex discriminating models developed through the PROC STEPWISE procedure relies heavily on measurements quantifying segments of the bone, rather than total length of the bone. The maximum epiphyseal breadth of the proximal tibia (MEP) also offers an adequate alternative to the use of tibial length to reconstruct stature in males. Following the maximum length of the tibia (MLT) and the length of the tibia (L0T), this measurement consistently provides the best explanation of stature variation as it is represented by the male calibration samples. This demonstrates the applicability of measurements such as the maximum epiphyseal breadth of the proximal tibia (MEP)

to the investigation of human variation, and supports the suggestion that further research should focus on using measurements that do not necessitate complete skeletal materials.

The inclusion of the length from the intercondylar eminence to the nutrient foramen (LIN) in this study provided support for the claims that the location of nutrient foramen varies (Kizilkanat et al., 2007). This measurement also proved useful in the identification of the sex of an individual in that it was employed in multiple sex discriminating models. It is suggested that further investigation utilizing this measurement will aid in explaining the variability of nutrient foramina, especially how it varies between the sexes. It also confirms the efficacy of the quantification of areas and features of the tibia in the investigation of human variation.

Summary

This study is comprised of multiple objectives all addressing the same topic of human variation. Through univariate and multivariate analyses the degree of variation at the individual and population level was addressed with respect to the implications of sex and age on this variation. Further, the degree to which the morphological variation of the human tibia aids in the explanation of living stature was also explored. Utilizing traditional and non-traditional quantification techniques each of these objectives was assessed and discussed.

Evaluating the correlation of tibial dimensions revealed the covariance of multiple dimensions. Overall, it was identified that multiple dimensions possess strong positive correlation which aids in the understanding of how the tibia varies within the individual. These correlations also suggest that measurements responsible for quantifying similar features or locations may be interchangeable pending further investigation. Should this be the case, the ability of anthropologists to quantify and assess fragmentary remains will be greatly impacted. The longitudinal analysis of these correlations may provide insight into spatial and temporal variation, and therefore should be undertaken to do so.

The results of this study also highlight the morphological differences represented by the tibial dimensions among and between the sexes, as well as in respect to their corresponding age groups. Not

only are the shape and size variations between the samples discerned, but the ability of the dimensions to accurately discriminate the sex of an individual is identified. Specifically, this study provides support and further clarification of the use of the proximal end of the tibia in sex estimation. The maximum epiphyseal breadth of the proximal tibia (MEP) continuously provides accurate estimations of sex in both males and females, in addition to all age groups. Further investigation concerning the applicability of this dimension to assess the variability between the sexes of different group affiliations should be addressed before it is applied to skeletal remains other than those designated as Black Americans.

The interaction of the tibial morphology and stature revealed, as expected, that the best indicators of stature are those dimensions incorporating the total length of the long bone. Within the male calibration samples, the maximum epiphyseal breadth of the proximal tibia (MEP) provides the next best predictor of stature. This trend is not observed in the female sample, and it is proposed that secular variation within the females is so profound that it impeded the results associated with stature reconstruction. To this end, additional research is required from a sample that enables the restriction of birth cohorts in both females and males to adequately assess the capability of the maximum epiphyseal breadth of the proximal tibia (MEP) to explain stature, as well as the other measurements implemented in this study. The accuracy of each of the dimensions in reconstructing stature should also be addressed within this sample, in addition to samples involving different group affiliations.

This study also attests to the usefulness of quantification methods that do not rely on complete skeletal remains. Not only was it revealed that multiple measurements, especially the maximum epiphyseal breadth of the proximal tibia (MEP), provide accurate representations of the variation expressed by both sexes and their corresponding age groups, but it was also demonstrated that, when necessary, particular measurements may be interchangeable due to their strong correlations with one another. Further exploration into both of these issues could prove invaluable in the obtainment of data from fragmentary or damaged skeletal remains, allowing for a more inclusive representation of past and present human variation.

BIBLIOGRAPHY

BIBLIOGRAPHY

Acheson, RM
1960 Effects of Nutrition and Disease on Human Growth: In Human Growth. Oxford: Pergamon.

Aiello L, Dean C
1990 An Introduction to Human Evolutionary Anatomy. London: Academic Press.

Borkan GA, Hults DE, Glynn RJ
1983 Role of Longitudinal Change and Secular Trend in Age Differences in Male Body Dimensions. Human Biology, 55:629-641.

Buffa R, Marini E, Floris G
2001 Variation in Sexual Dimorphism in Relation to Physical Activity. American Journal of Human Biology, 13:341-348.

Cobb WM
1932 Human Archives. Ph.D. Dissertation, Department of Anatomy, Western Reserve University.

de la Cova C
2011 Race, Health, and Disease in 19th-Century-Born Males. American Journal of Physical Anthropology, 144: 526-537.

Delwiche LD, Slaughter SJ
2008 The Little SAS Book: A Primer, 4th ed. Cary: SAS Institute Inc.

Drapeau M, Streeter MA
2006 Modeling and Remodeling Responses to Normal Loading in the Human Lower Limb. American Journal of Physical Anthropology, 129: 403-409.

Droessler J
1981 Crainometry and Biological Distance. Evanston, IL: Center for American Archaeology at Northwestern University, Research Series, Volume 1.

Duyar I, Pelin C
2003 Body Height Estimation Based on Tibia Length in Different Stature Groups. American Journal of Physical Anthropology, 122:23-27

Dwight T
1894 Methods of Estimating the Height From Parts of the Skeleton. New York: Trow Directory, Printing, and Bookbinding CO.

Eveleth PB
1975 Differences Between Ethnic Groups in Sex Dimorphism of Adult Height. Annals of Human Biology, 1975:35-39.

Frayer DW, Wolpoff MH
1985 Sexual Dimorphism. The Annual Review of Anthropology, 14:429-473.

Giles E
1991 Corrections for Age in Estimating Older Adults' Stature from Long Bones. Journal of Forensic Sciences, 36: 898-901.

Gray JP, Wolfe LD
1980 Height and Sexual Dimorphism of Stature Among Human Societies. American Journal of Physical Anthropology, 53:441-456.

Gray H
2010 Anatomy Descriptive and Surgical, 15th ed. New York: Barnes and Noble.

Guggenbuhl P
2009 Osteoporosis in Males and Females: Is there Really a Difference? Joint Bone Spine, 76:595-601.

Holland, TD
1991 Sex Assessment Using the Proximal Tibia. American Journal of Physical Anthropology, 85:221-227.
1992 Estimation of Adult Stature from Fragmentary Tibias. Journal of Forensic Sciences. 37: 1223-1229.

İşcan MY
1990 A Comparison of Techniques On the Determination of Race, Sex, and Stature from the Terry and Hamann-Todd Collections. In Gill GW, Rhine JS (eds): Skeletal Attribution of Race: Methods in Forensic Anthropology. Albuquerque: University of New Mexico, 73-80.

İşcan MY, Miller-Shaivitz P
1984 Determination of Sex From the Tibia. American Journal of Physical Anthropology, 64: 53-57.

Jacobs K
1992 Estimating Femur and Tibia Length from Fragmentary Bones: an Evaluation of Steele's (1970) Method Using a Prehistoric European Sample. American Journal of Physical Anthropology, 89:333-345.

Jacobs SW, Francone CA, Walter JL
1978 Structure and Function in Man. Philadelphia: WB Saunders Company.

Jaeger, RM
1993 Statistics: A Spectator Sport. Newbury Park: Sage Publications.

Jantz, RL
1992 Modification of the Trotter and Gleser Female Stature Estimation Formulae. Journal of Forensic Sciences, 37:1230-1235

Jantz LM, Jantz RL
1994 Maximum Length of the Tibia: How did Trotter Measure it. American Journal of Physical Anthropology, 93: 525-528.
1995 The Measure and Mismeasure of the Tibia: Implications for Stature Estimation. Journal of Forensic Sciences, 40:758-761
1995 Allometic Secular Change in the Long Bones from the 1800's to the Present. Journal of Forensic Sciences, 40: 762-767
1999 Secular Change in Long Bone Length and Proportion in the United States, 1800-1970. American Journal of Physical Anthropology, 110:57-67.

Jones-Kern K , Latimer, B
1996 Skeletons Out of the Closet. The Explorer, 38:26-28.

Keen EN
1953 Estimation of Stature from the Long Bones. Journal of Forensic Medicine, 1:46-51.

Kelley MA, El-Najjar MY
1980 Natural Variation and Differential Diagnosis of Skeletal Changes in Tuberculosis. American Journal of Physical Anthropology, 52:153-167.

Kizilkanat E, Boyan N, Ozsahin ET, Soames R, Oguz O
2007 Location, Number and Clinical Significance of Nutrient Foramina in Human Long Bones. Annals of Anatomy, 189:87-95.

Kozac J
1996 Stature Reconstruction from Long Bones. The Estimation of the Usefulness of Some Selected Methods for Skeletal Populations from Poland. Variability and Evolution, 5: 83-94.

Krogman WM, İşcan MY
1986. The Human Skeleton in Forensic Medicine. Springfield: C. C. Thomas.

Kurki HK, Ginter JK, Stock JT, Pfeiffer S
2010 Body Size Estimation of Small-Bodied Humans: Applicability of Current Methods. American Journal of Physical Anthropology, 141: 169-180.

Larsen CS
2000 Bioarchaeology: Interpreting Behavior from the Human Skeleton. Chapel Hill: Cambridge University Press.

Loeser, Richard F
2010 Age-Related Changes in the Musculoskeletal System and the Development of Osteoarthritis. Clinics in Geriatric Medicine, 26:371-386.

Loeser RF, Shakoor N
2003 Aging or Osteoarthritis: Which is the Problem? Rheumatic Disease Clinics of North America, 29:653-673.

Nath S, Kaur S, Jain P
1998 Determination of Stature from Fragmentary Dimensions of Male Tibia. Indian Journal of Physical Anthropology and Human Genetics, 21:135-140.

Manolagas, Stavros C, and A. Michael Parfitt
2010 What Old Means to Bone. Trends in Endocrinology and Metabolism, 21:369-374.

Meadows L, Jantz, RL
1995 Allometric Secular Change in the Long Bones from the 1800's to the Present. Journal of Forensic Science, 40:762-767.

Meredith, HV
1976 Findings from Asia, Australia, Europe, and North America on Secular Changes in Mean Height of Children, Youths, and Young Adults. American Journal of Physical Anthropology, 44:315-326.

Moore-Jansen PH.
1989 A Multivariate Craniometric Analysis of Secular Change and Variation Among Recent North American Populations. Ph. D. Dissertation, Department of Anthropology, University of Tennessee, Knoxville.

Moore-Jansen PH, Ousley SD, Jantz RL
1994 Data Collection Procedures for Forensic Skeletal Material, 3rd Ed. Knoxville: University of Tennessee Forensic Anthropology Series.

Ortner DJ
2003 Identifications of Pathological Conditions in Human Skeletal Remains. 2nd Ed. Amsterdam: Academic Press.

Pearson K
1899 Mathematical Contributions to the Theory of Evolution. V. On the Reconstruction of the Stature of Prehistoric Faces. Philosophical Transactions of the Royal Society of London. Series A. Containing Papers of Mathematical or Physical Character 192: 169-244.

Price B, Cameron N, Tobias PV
1987 A Further Search for a Secular Trend of Adult Body Size in South African Blacks: Evidence from the Femur and Tibia. Human Biology, 59:467-475.

Raxter MH, Auerbach BM, Ruff CB
2006 Revision of the Fully Technique for Estimating Statures. American Journal of Physical Anthropology 130:374-384.

Rang M
1969 The Growth Plate and its Disorders. Edinburgh: E. & S. Livingstone LTD.

Relethford J H, Lees FC
1981 The Effects of Aging and Secular Trend on Adult Stature in Rural Western Ireland. American Journal of Physical Anthropology, 55:81-88.

Safont S, Malgosa A, Subira ME
2000 Sex Assessment on the Basis of Long Bone Circumference. American Journal of Physical Anthropology, 113:317-328.

SAS Institue Inc.
1985 SAS User's Guide: Statistics, Version 5 Edition. Cary, NC: SAS Institute Inc.
1999 Getting Started with the SAS System, Version 8. Cary, NC: SAS Institute Inc.

Schwartz JH
1995 Skeleton Keys: an Introduction to Human Skeletal Morphology, Development and Analysis. New York: Oxford University Press.

Scheuer L, Black S
2000 Developmental Juvenile Osteology. Amsterdam: Elsevier Academic Press.
2004 The Juvenile Skeleton. London: Elsevier Academic Press.

Shaw CN, Stock JT
2011 The Influence of Body Proportions on Femoral and Tibial Midshaft Shape in Hunter-Gathers. American Journal of Physical Anthorpology, 144:22-29

Steele DG
1970 Estimation of Stature From Fragments of Long Limb Bones. In: Stewart TD editor. Personal Identification in mass disasters. Washington DC: Smithsonian Institution. p85-97.Steele DG, Bramblett CA.

1988 The anatomy and biology of the human skeleton. College Station: Texas A & M University Press.

Steele DG, McKern TW
1969 A Method for Assessment of Maximum Long Bone Length and Living Stature from Fragmentary Long Bones. American Journal of Physical Anthropology, 31:215-228.

Stevens SD, Vidarsdottir US
2008 Morphological Changes in the Shape of the Non-pathological Bony Knee Joint with Age: A Morphometic Analysis of the Distal Femur and Proximal Tibia in Three Populations of Known Age at Death. International Journal of Osteoarchaeology, 18:352-371.

Todd TW, Lindala A
1928 Dimensions of the Body: Whites and American Negroes of Both Sexes. American Journal of Physical Anthropology, 12:35-119.

Trotter M, Gleser GC
1951 The Effects of Aging on Stature. American Journal of Physical Anthropology, 9:311-324.
1952 Estimation of Stature from Long Bones of American Whites and Negroes. American Journal of Physical Anthropology, 10:463-514.
1958 A Re-evaluation of Estimation of Stature Based on Measurements of Stature Taken During Life and Long Bones After Death. American Journal of Physical Anthropology, 16:79-123.

Ubelaker DH
1978 Human Skeletal Remains: Excavation, Analysis, Interpretation. Washington:Smithsonian Institution.

Vercellotti G, Agnew AM, Justus HM, Sciulli PW
2009 Stature Estimation in an Early Medieval (XI-XII c.) Polish population: Testing the Accuracy of Regression Equations in Bioarcheaolgical Sample. American Journal of Physical Anthropology, 140:135-142.

Voisin MD
2011 Sexual Dimorphism in the 12th Thoracic Vertebra and its Potential for Sex Estimation. M.A. Thesis, Department of Anthropology, Wichita State University.

Waxenbaum EB, Hunt DR, Falsetti AB
2010 Intercondylar Eminences and their Effect on the Maximum Length Measure of the Tibia. Journal of Forensic Sciences, 55:145-148.

White TD
2000 Human osteology, 2nd ed. San Diego: Academic Press.

Wright LE, Vasquz MA
2003 Estimating the Length of Incomplete Long Bones Forensic Standards from Guatemala. American Journal of Physical Anthropology, 120:233-251.

APPENDICIES

APPENDIX A

DEMONSTRATION OF MEASUREMENTS

1. Maximum length of the tibia (MLT)

This measurement is taken using an osteometric board and recorded in millimeters. The measurement is defined as the distance between the most proximal point of the intercondylar eminence to the medial malleolus.

2. Length of the tibia (L0T)

This measurement is taken using an osteometric board and recorded in millimeters. The measurement is defined as "the distance from the superior articular surface of the lateral condyle of the tibia to the tip of the medial malleolus" (Moore-Jansen et al. 1994).

3. Maximum epiphyseal breadth of the proximal tibia (MEP)

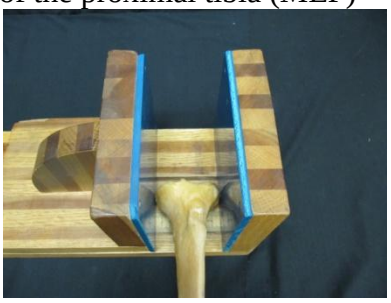

This measurement is taken using an osteometric board and recorded in millimeters. The measurement is defined as "the maximum distance between the two most laterally projecting points on the medial and lateral condyles of the proximal epiphysis" (Moore-Jansen et al. 1994).

4. Maximum epiphyseal breadth of the distal tibia (MED)

This measurement is taken using an osteometric board and recorded in millimeters. The measurement is defined as "the distance between the two most medial points on the medial malleolus and the lateral surface of the distal epiphysis" (Moore-Jansen et al. 1994).

5. Anterior/Posterior epiphyseal breadth of the distal tibia (AED)

This measurement is taken using an osteometric board and recorded in millimeters. The measurement is defined as the maximum distance between the anterior and posterior borders of the distal epiphysis.

6. Maximum diameter of the tibia at the nutrient foramen (MDN)

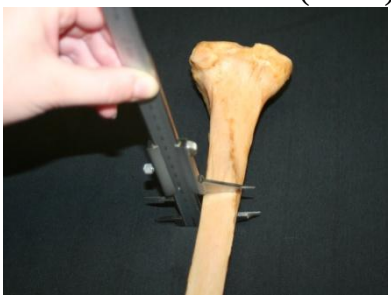

This measurement is taken using a sliding caliper and recorded in millimeters. The measurement is defined as "the distance between the anterior crest and the posterior surface at the level of the nutrient foramen" (Moore-Jansen et al. 1994).

7. Transverse diameter of the tibia at the nutrient foramen (TDN)

This measurement is taken using a sliding caliper and recorded in millimeters. The measurement is defined as the distance between the medial and lateral margins at the level of the nutrient foramen (Moore-Jansen et al. 1994).

8. Maximum diameter of the tibia at the midshaft (MDM)

This measurement is taken using a sliding caliper and recorded in millimeters. The measurement is defined as the maximum diameter at the measured midshaft.

9. Transverse diameter of the tibia at the midshaft (TDM)

This measurement is taken using a sliding caliper and recorded in millimeters. The measurement is defined as distance between the medial and lateral margins at the measured midshaft.

10. Length from intercondylar eminence to the nutrient foramen (LIN)

This measurement is taken using a sliding caliper and recorded in millimeters. The measurement is defined as distance from the intercondylar eminence down to the nutrient foramen.

11. Circumference of the tibia at the nutrient foramen (C0N)

This measurement is taken using fiberglass tape and recorded in millimeters. The measurement is defined as "the circumference measured at the level of the nutrient foramen" (Moore-Jansen et al. 1994)

12. Circumference of the tibia at the midshaft (C0M)

This measurement is taken using fiberglass tape and recorded in millimeters. The measurement is defined as the circumference obtained at the measured midshaft.

APPENDIX B

DATA COLLECTION FORMS

Observer: Shannon Arney **Date:** 02/ /2011 **Page___ of ___**

ID#:________ H-T#: ________ Age: ________ Sex: ________ Cadaver Height: ________

Tibial Measurements (mm)

1. MLT ________	7. TDN ________	Notes:________________________________
2. L0T ________	8. MDM ________	________________________________
3. MEP ________	9. TDM ________	________________________________
4. MED ________	10. LIN ________	________________________________
5. AED ________	11. C0N ________	________________________________
6. MDN ________	12. C0M ________	

ID#:________ H-T#: ________ Age: ________ Sex: ________ Cadaver Height: ________

Tibial Measurements (mm)

1. MLT ________	7. TDN ________	Notes:________________________________
2. L0T ________	8. MDM ________	________________________________
3. MEP ________	9. TDM ________	________________________________
4. MED ________	10. LIN ________	________________________________
5. AED ________	11. C0N ________	________________________________
6. MDN ________	12. C0M ________	

ID#:________ H-T#: ________ Age: ________ Sex: ________ Cadaver Height: ________

Tibial Measurements (mm)

1. MLT ________	7. TDN ________	Notes:________________________________
2. L0T ________	8. MDM ________	________________________________
3. MEP ________	9. TDM ________	________________________________
4. MED ________	10. LIN ________	________________________________
5. AED ________	11. C0N ________	________________________________
6. MDN ________	12. C0M ________	

APPENDIX C

UNIVARIATE SUMMARY STATISTICS

Table 37. Tibial Measurements - Total Sample (n =383)

Code	Measurement	Mean	Var.	St. Dev.	Range
MLT	Maximum length of the tibia	386.4	852.5	29.2	290.0 – 470.0
L0T	Length of the tibia	377.3	822.1	28.7	251.0 – 444.0
MEP	Maximum epiphyseal breadth of the proximal tibia	75.6	34.4	5.9	60.0 – 89.0
MED	Maximum epiphyseal breadth of the distal tibia	47.2	20.7	4.5	35.0 – 80.0
AED	Anterior/Posterior epiphyseal breadth of the distal tibia	40.0	13.1	3.6	27.2 – 55.0
MDN	Maximum diameter of the tibia at the nutrient foramen	33.6	13.0	3.6	22.6 – 48.4
TDN	Transverse diameter of the tibia at the nutrient foramen	24.8	8.5	2.9	18.1 – 36.4
MDM	Maximum diameter of the tibia at the midshaft	29.0	12.3	3.5	16.3 – 39.6
TDM	Transverse diameter of the tibia at the midshaft	22.1	8.6	2.9	16.0 – 33.6
LIN	Length from intercondylar eminence to the nutrient foramen	120.3	180.7	13.4	84.2 – 152.5
C0N	Circumference of the tibia at the nutrient foramen	93.5	76.2	8.7	75.0 - 121.0
C0M	Circumference of the tibia at the midshaft	82.3	61.9	7.9	41.0 – 104.0

Table 38. Tibial Measurements – Female Sample (n = 180)

Code	Measurement	Mean	Var.	St. Dev.	Range
MLT	Maximum length of the tibia	368.3	550.3	23.5	290.0 – 470.0
L0T	Length of the tibia	359.0	536.6	23.2	251.0 – 416.0
MEP	Maximum epiphyseal breadth of the proximal tibia	70.8	13.5	3.7	60.0 – 80.0
MED	Maximum epiphyseal breadth of the distal tibia	44.1	8.1	2.8	35.0 – 59.0
AED	Anterior/Posterior epiphyseal breadth of the distal tibia	37.5	5.8	2.4	31.0 – 46.0
MDN	Maximum diameter of the tibia at the nutrient foramen	31.4	5.9	2.4	22.6 – 37.0
TDN	Transverse diameter of the tibia at the nutrient foramen	23.2	5.5	2.3	18.1 – 33.1
MDM	Maximum diameter of the tibia at the midshaft	26.8	7.5	2.7	18.7 – 39.1
TDM	Transverse diameter of the tibia at the midshaft	20.7	6.9	2.6	16.0 – 30.7
LIN	Length from intercondylar eminence to the nutrient foramen	113.6	138.7	11.8	84.2 – 144.3
C0N	Circumference of the tibia at the nutrient foramen	87.4	36.8	6.1	75.0 – 102.0
C0M	Circumference of the tibia at the midshaft	76.9	27.0	5.2	66.0 – 89.0

Table 39. Tibial Measurements – Male Sample (n = 202)

Code	Measurement	Mean	Var.	St. Dev.	Range
MLT	Maximum length of the tibia	402.6	567.5	23.8	328.0 – 470.0
L0T	Length of the tibia	393.6	513.8	22.7	323.0 – 444.0
MEP	Maximum epiphyseal breadth of the proximal tibia	79.9	14.0	3.7	71.0 – 89.0
MED	Maximum epiphyseal breadth of the distal tibia	50.0	15.5	3.9	38.6 – 80.0
AED	Anterior/Posterior epiphyseal breadth of the distal tibia	42.2	9.3	3.0	27.2 – 55.0
MDN	Maximum diameter of the tibia at the nutrient foramen	35.7	10.6	3.3	23.3 – 48.4
TDN	Transverse diameter of the tibia at the nutrient foramen	26.3	6.5	2.5	19.3 – 36.4
MDM	Maximum diameter of the tibia at the midshaft	30.9	8.5	2.9	16.3 – 39.6
TDM	Transverse diameter of the tibia at the midshaft	23.5	6.8	2.6	17.3 – 33.6
LIN	Length from intercondylar eminence to the nutrient foramen	126.2	143.2	12.0	89.0 – 152.5
C0N	Circumference of the tibia at the nutrient foramen	98.8	50.0	7.1	78.0 – 121.0
C0M	Circumference of the tibia at the midshaft	87.0	44.8	6.7	41.0 – 104.0

Table 40. Tibial Measurements with Ages – Female Sample (n = 180)

Code	Measurement	Age	Mean	Var.	St. Dev.	Range
MLT	Maximum length of the tibia	≤ 40	370.2	463.7	21.5	323.0 – 423.0
		> 40	366.2	636.9	25.2	290.0 – 470.0
L0T	Length of the tibia	≤ 40	361.1	566.2	23.8	251.0 – 416.0
		> 40	357.0	503.9	22.4	283.0 – 414.0
MEP	Maximum epiphyseal breadth of the proximal tibia	≤ 40	69.9	11.3	3.4	60.0 – 77.0
		> 40	71.7	14.5	3.8	63.0 – 80.0
MED	Maximum epiphyseal breadth of the distal tibia	≤ 40	43.5	6.3	2.5	35.0 – 49.0
		> 40	44.7	9.2	3.0	39.0 – 59.0
AED	Anterior/Posterior epiphyseal breadth of the distal tibia	≤ 40	37.2	5.6	2.4	32.0 – 46.0
		> 40	37.8	5.9	2.4	31.0 – 42.0
MDN	Maximum diameter of the tibia at the nutrient foramen	≤ 40	31.0	5.7	2.4	25.5 – 37.0
		> 40	31.7	5.9	2.4	22.6 – 36.3
TDN	Transverse diameter of the tibia at the nutrient foramen	≤ 40	23.3	6.4	2.5	18.1 – 33.1
		> 40	23.0	4.6	2.1	18.2 – 28.4
MDM	Maximum diameter of the tibia at the midshaft	≤ 40	26.8	4.4	2.1	20.3 – 32.4
		> 40	26.8	10.7	3.3	18.7 – 39.1
TDM	Transverse diameter of the tibia at the midshaft	≤ 40	20.2	4.4	2.1	16.0 – 29.5
		> 40	21.1	8.6	2.9	16.8 – 30.7
LIN	Length from intercondylar eminence to the nutrient foramen	≤ 40	113.6	133.7	11.6	88.8 – 143.0
		> 40	113.6	145.4	12.1	84.2 – 144.3
C0N	Circumference of the tibia at the nutrient foramen	≤ 40	86.8	36.6	6.0	75.0 - 101.0
		> 40	88.1	36.5	6.0	75.0 – 102.0
C0M	Circumference of the tibia at the midshaft	≤ 40	76.1	23.4	4.8	101.0 – 88.0
		> 40	77.8	5.4	29.4	67.0 – 89.0

Table 41. Tibial Measurements with Ages – Male Sample (n = 202)

Code	Measurement	Age	Mean	Var.	St. Dev.	Range
MLT	Maximum length of the tibia	≤ 40	401.4	546.1	23.4	328.0 – 454.0
		> 40	403.8	592.1	24.3	332.0 – 470.0
L0T	Length of the tibia	≤ 40	393.1	510.0	22.6	323.0 – 444.0
		> 40	394.2	522.2	22.9	324.0 – 439.0
MEP	Maximum epiphyseal breadth of the proximal tibia	≤ 40	79.4	12.9	3.6	71.0 – 89.0
		> 40	80.4	14.9	3.9	71.0 – 89.0
MED	Maximum epiphyseal breadth of the distal tibia	≤ 40	50.0	19.2	4.4	42.0 – 80.0
		> 40	50.0	11.8	3.4	38.6 – 59.0
AED	Anterior/Posterior epiphyseal breadth of the distal tibia	≤ 40	41.8	6.3	2.5	36.0 – 49.0
		> 40	42.6	12.0	3.5	27.2 – 55.0
MDN	Maximum diameter of the tibia at the nutrient foramen	≤ 40	35.2	9.1	3.0	23.3 – 42.1
		> 40	36.1	11.8	3.4	26.2 – 48.4
TDN	Transverse diameter of the tibia at the nutrient foramen	≤ 40	26.4	5.3	2.3	21.5 – 33.7
		> 40	26.2	7.7	2.8	19.3 – 36.4
MDM	Maximum diameter of the tibia at the midshaft	≤ 40	30.6	7.6	2.8	21.7 – 37.4
		> 40	31.3	9.2	3.0	16.3 – 39.6
TDM	Transverse diameter of the tibia at the midshaft	≤ 40	23.4	6.4	2.5	18.1 – 33.6
		> 40	23.6	7.1	2.7	17.3 – 32.1
LIN	Length from intercondylar eminence to the nutrient foramen	≤ 40	126.9	169.2	13.0	96.8 – 152.5
		> 40	125.6	117.2	10.8	89.0 – 152.3
C0N	Circumference of the tibia at the nutrient foramen	≤ 40	98.0	48.7	7.0	78.0 – 121.0
		> 40	99.7	50.5	7.1	81.0 – 121.0
C0M	Circumference of the tibia at the midshaft	≤ 40	86.2	30.2	5.5	76.0 – 104.0
		> 40	88.0	58.5	7.7	41.0 – 100.0

APPENDIX D

PEARSON PRODUCT MOMENT CORRELATIONS

Table 42. Pearson product moment correlations between tibial measurements in the pooled test sample

	MLT	L0T	MEP	MED	AED	MDN	TDN	MDM	TDM	LIN	C0N	C0M
MLT	1.0000	0.9274	0.7280	0.5229	0.6306	0.6006	0.6023	0.4741	0.6186	0.7083	0.6717	0.6312
L0T	<.0001	1.0000	0.7280	0.5357	0.6374	0.6275	0.6048	0.5176	0.5701	0.7060	0.6874	0.6440
MEP	<.0001	<.0001	1.0000	0.7586	0.7254	0.6293	0.6209	0.5690	0.5600	0.5835	0.7336	0.7137
MED	<.0001	<.0001	<.0001	1.0000	0.6108	0.4797	0.4870	0.4203	0.3956	0.4302	0.5654	0.5140
AED	<.0001	<.0001	<.0001	<.0001	1.0000	0.4678	0.4807	0.4449	0.4840	0.6185	0.5240	0.5730
MDN	<.0001	<.0001	<.0001	<.0001	<.0001	1.0000	0.6200	0.6257	0.5722	0.3476	0.8642	0.8165
TDN	<.0001	<.0001	<.0001	<.0001	<.0001	<.0001	1.0000	0.4037	0.6674	0.3566	0.7937	0.6494
MDM	<.0001	<.0001	<.0001	<.0001	<.0001	<.0001	<.0001	1.0000	0.1994	0.3845	0.6393	0.6796
TDM	<.0001	<.0001	<.0001	<.0001	<.0001	<.0001	<.0001	0.0173	1.0000	0.4915	0.6473	0.6758
LIN	<.0001	<.0001	<.0001	<.0001	<.0001	<.0001	<.0001	<.0001	<.0001	1.0000	0.3765	0.4818
C0N	<.0001	<.0001	<.0001	<.0001	<.0001	<.0001	<.0001	<.0001	<.0001	<.0001	1.0000	0.8476
C0M	<.0001	<.0001	<.0001	<.0001	<.0001	<.0001	<.0001	<.0001	<.0001	<.0001	<.0001	1.0000

Values are significant at $\alpha < .05$

Table 43. Pearson product moment correlations between tibial measurements in the female test sample

	MLT	L0T	MEP	MED	AED	MDN	TDN	MDM	TDM	LIN	C0N	C0M
MLT	1.0000	0.7895	0.5331	0.4033	0.5237	0.3125	0.3671	0.1484	0.6183	0.6279	0.4129	0.3343
L0T	<.0001	1.0000	0.4420	0.3172	0.4952	0.3429	0.2772	0.2414	0.3630	0.5776	0.3800	0.2826
MEP	<.0001	0.0004	1.0000	0.6171	0.5708	0.4241	0.3276	0.2852	0.4191	0.3886	0.5721	0.4495
MED	0.0014	0.0135	<.0001	1.0000	0.4355	0.3179	0.1673	0.1746	0.3310	0.3202	0.4212	0.3401
AED	<.0001	<.0001	<.0001	0.0005	1.0000	0.2325	0.3188	0.1180	0.3817	0.4980	0.3941	0.3945
MDN	0.0160	0.0078	0.0008	0.0141	0.0764	1.0000	0.3294	0.4589	0.3296	0.0342	0.8064	0.7438
TDN	0.0039	0.0320	0.0106	0.2013	0.0130	0.0108	1.0000	0.12635	0.4562	0.2066	0.6632	0.3000
MDM	0.2577	0.0632	0.0272	0.1820	0.3691	0.0003	0.3361	1.0000	-.01359	0.1551	0.4518	0.4014
TDM	0.6183	0.0044	0.0009	0.0098	0.0026	0.0108	0.0002	-0.1359	1.0000	0.3775	0.4501	0.4480
LIN	<.0001	<.0001	0.0022	0.0126	<.0001	0.7971	0.1132	0.2368	0.0029	1.0000	0.1170	0.1835
C0N	0.0010	0.0027	<.0001	0.0008	0.0018	<.0001	<.0001	0.003	0.0003	0.3735	1.0000	0.7245
C0M	0.0090	0.0286	0.0003	0.0078	0.0018	<.0001	0.0199	0.0015	0.0003	0.1604	<.0001	1.0000

Values are significant at $\alpha < .05$

Table 44. Pearson product moment correlations between tibial measurements in the male test sample

	MLT	L0T	MEP	MED	AED	MDN	TDN	MDM	TDM	LIN	C0N	C0M
MLT	1.0000	0.9589	0.5812	0.2604	0.4166	0.4730	0.5053	0.3253	0.4068	0.5473	0.5420	0.4846
L0T	<.0001	1.0000	0.5932	0.2998	0.4181	0.5007	0.5465	0.3420	0.4386	0.5529	0.5730	0.5155
MEP	<.0001	<.0001	1.0000	0.6365	0.5297	0.3928	0.5034	0.3571	0.3229	0.2721	0.5114	0.5066
MED	0.0182	0.0062	<.0001	1.0000	41640	0.2241	0.3525	0.1940	0.1150	0.1130	0.3075	0.2206
AED	<.0001	<.0001	<.0001	<.0001	1.0000	0.2025	0.2418	0.2449	0.2526	0.4125	0.1987	0.2961
MDN	<.0001	<.0001	0.0003	0.0430	0.0681	1.0000	0.5497	0.4878	0.4772	0.0822	0.7945	0.7187
TDN	<.0001	<.0001	<.0001	0.0012	0.0287	<.0001	1.0000	0.2373	0.6339	0.0518	0.7431	0.6060
MDM	0.0029	0.0017	0.0010	0.0808	0.0266	<.0001	0.0318	1.0000	-0.0082	0.1309	0.4908	0.6051
TDM	0.001	<.0001	0.0031	0.3035	0.0220	<.0001	<.0001	0.9419	1.0000	0.2809	0.5505	0.6131
LIN	<.0001	<.0001	0.0134	0.3120	0.001	0.4629	0.6441	0.2411	0.0106	1.0000	0.0263	0.2260
C0N	<.0001	<.0001	<.0001	0.0050	0.0736	<.0001	<.0001	<.0001	<.0001	0.8143	1.0000	0.7634
C0M	<.0001	<.0001	<.0001	0.0464	0.0069	<.0001	<.0001	<.0001	<.0001	0.0412	<.0001	1.0000

Values are significant at $\alpha < .05$

Table 45. Pearson product moment correlations between tibial measurements in the young adult female test sample

	MLT	L0T	MEP	MED	AED	MDN	TDN	MDM	TDM	LIN	C0N	C0M
MLT	1.0000	0.7682	0.4941	0.4553	0.5086	0.4570	0.4422	0.3326	0.5782	0.6513	0.5236	0.4257
L0T	<.0001	1.0000	0.2939	0.2354	0.3960	0.4274	0.2232	0.2728	0.2811	0.4774	0.3729	0.2950
MEP	0.0047	0.1085	1.0000	0.6700	0.4697	0.2299	0.2174	0.4091	0.1826	0.3027	0.3995	0.2867
MED	0.0101	0.2024	<.0001	1.0000	0.2807	0.3241	0.2400	0.3717	0.2618	0.2152	0.4981	0.2545
AED	0.0035	0.0274	0.0077	0.1261	1.0000	0.1162	0.1619	0.2458	0.2717	0.4565	0.2346	0.4106
MDN	0.0111	0.0185	0.2216	0.0806	0.5408	1.0000	0.1806	0.6145	0.3719	0.0069	0.7192	0.6142
TDN	0.0128	0.2275	0.2401	0.1935	0.3843	0.3396	1.0000	0.0905	0.7210	0.2764	0.5733	0.2568
MDM	0.0676	0.1376	0.0223	0.0395	0.1826	0.0003	0.6281	1.0000	0.1019	0.1574	0.6460	0.5938
TDM	0.0007	0.1256	0.3255	0.1548	0.1393	0.0430	<.0001	0.5853	1.0000	0.3333	0.5981	0.3695
LIN	<.0001	0.0066	0.0979	0.2451	0.0099	0.9713	0.1323	0.3977	0.0669	1.0000	0.0697	0.138
C0N	0.0025	0.0388	0.0260	0.0043	0.2039	<.0001	0.0007	<.0001	0.0004	0.7096	1.0000	0.6513
C0M	0.0170	0.1072	0.1179	0.1671	0.0218	0.0003	0.1631	0.0004	0.0408	0.4582	<.0001	1.0000

Values are significant at $\alpha < .05$

Table 46. Pearson product moment correlations between tibial measurements in the young adult male test sample

	MLT	L0T	MEP	MED	AED	MDN	TDN	MDM	TDM	LIN	C0N	C0M
MLT	1.0000	0.9921	0.6286	0.2068	0.4398	0.5237	0.5205	0.3507	0.5125	0.5197	0.5691	0.4375
L0T	<.0001	1.0000	0.6202	0.2256	0.4336	0.4945	0.4826	0.3538	0.4804	0.5401	0.5505	0.4207
MEP	<.0001	<.0001	1.0000	0.5734	0.5705	0.3402	0.4549	0.3741	0.1927	0.2120	0.4716	0.4346
MED	0.1889	0.1508	<.0001	1.0000	0.3371	0.1830	0.2667	0.1799	-0.0467	-0.0173	0.2978	0.1155
AED	0.0036	0.0041	<.0001	0.0290	1.0000	0.2876	0.1210	0.2741	0.0836	0.2914	0.2270	0.1541
MDN	0.0004	0.0009	0.0275	0.2460	0.0647	1.0000	0.5458	0.6820	0.4860	0.0900	0.7782	0.7643
TDN	0.0004	0.0012	0.0025	0.0879	0.4452	0.0002	1.0000	0.3309	0.6866	-0.0633	0.7832	0.5573
MDM	0.0228	0.0215	0.0147	0.2543	0.0790	<.0001	0.0323	1.0000	0.0801	0.1446	0.6735	0.7943
TDM	0.0005	0.0013	0.2214	0.7691	0.5987	0.0011	<.0001	0.6143	1.0000	0.1996	0.5126	0.4678
LIN	0.0004	0.0002	0.1778	0.9137	0.0612	0.5709	0.6907	0.3610	0.2050	1.0000	-0.0578	0.1359
C0N	<.0001	0.0002	0.0016	0.0555	0.1482	<.0001	<.0001	<.0001	0.0005	0.7160	1.0000	0.7145
C0M	0.0038	0.0055	0.0040	0.4665	0.3300	<.0001	0.0001	<.0001	0.01018	0.3909	<.0001	1.0000

Values are significant at $\alpha < .05$

Table 47. Pearson product moment correlations between tibial measurements in the older adult female test sample

	MLT	L0T	MEP	MED	AED	MDN	TDN	MDM	TDM	LIN	C0N	C0M
MLT	1.0000	0.8932	0.6194	0.4252	0.5894	0.2512	0.3259	0.0915	0.6874	0.6357	0.3877	0.3028
L0T	<.0001	1.0000	0.7087	0.4838	0.6853	0.2868	0.3685	0.2808	0.5233	0.7425	0.4564	0.3097
MEP	0.0003	<.0001	1.0000	0.4959	0.6857	0.4247	0.4120	0.2298	0.4408	0.5750	0.6151	0.4706
MED	0.0215	0.0078	0.0062	1.0000	0.5710	0.1508	0.0708	0.0794	0.2482	0.5103	0.2415	0.2880
AED	0.0008	<.0001	<.0001	0,0012	1.0000	0.2859	0.5196	0.0435	0.4659	0.5969	0.5488	0.3455
MDN	0.1888	0.1314	0.0217	0.4349	0.1327	1.0000	0.4597	0.4241	0.1863	0.1298	0.8337	0.8110
TDN	0.0845	0.0492	0.0264	0.7153	0.0039	0.0121	1.0000	0.1491	0.2707	0.1370	0.7827	0.3207
MDM	0.4347	0.6370	0.1401	0.2306	0.8227	0.0219	0.4403	1.0000	-0.2622	0.1862	0.3951	0.3321
TDM	0.0151	<.0001	0.0036	0.0167	0.0109	0.3332	0.1556	0.1694	1.0000	0.5025	0.2654	0.4264
LIN	0.0007	0.0002	<.0001	0.0011	0.0006	0.5019	0.4784	0.3335	0.0055	1.0000	0.2315	0.2810
C0N	0.0580	0.0377	0.0128	0.0004	0.0021	<.0001	<.0001	0.0339	0.1641	0.2268	1.0000	0.7461
C0M	0.3347	0.1103	0.1021	0.0100	0.0664	<.0001	0.0898	0.0784	0.0211	0.1397	<.0001	1.0000

Values are significant at $\alpha < .05$

Table 48. Pearson product moment correlations between tibial measurements in the older adult male test sample

	MLT	L0T	MEP	MED	AED	MDN	TDN	MDM	TDM	LIN	C0N	C0M
MLT	1.0000	0.9237	0.5352	0.3735	0.4101	0.4177	0.4913	0.3082	0.3244	0.5846	0.5223	0.5511
L0T	<.0001	1.0000	0.5777	0.4587	0.4319	0.5219	0.6217	0.3469	0.4258	0.5728	0.6295	0.6597
MEP	0.0004	<.0001	1.0000	0.7962	0.4980	0.4501	0.5667	0.3351	0.4399	0.3580	0.5564	0.5756
MED	0.0176	0.0029	<.0001	1.0000	0.5939	0.3128	0.5253	0.2390	0.3602	0.3785	0.3357	0.4220
AED	0.0086	0.0054	0.0011	<.0001	1.0000	0.1116	0.3324	0.2096	0.3424	0.5467	0.1557	0.3862
MDN	0.0073	0.0006	0.0036	0.0494	0.4931	1.0000	0.5603	0.2977	0.4665	0.0684	0.8178	0.6616
TDN	0.0013	<.0001	0.0001	0.0005	0.0361	0.0002	1.0000	0.1594	0.5983	0.1830	0.7177	0.6667
MDM	0.0530	0.0283	0.0346	0.1376	0.1943	0.0621	0.3226	1.0000	-0.0979	0.1189	0.3006	0.4354
TDM	0.0411	0.0062	0.0045	0.0224	0.0305	0.0024	<.0001	0.5477	1.0000	0.3732	0.6016	0.7279
LIN	<.0001	0.0001	0.0233	0.0160	0.0003	0.6751	0.2584	0.4648	0.37322	1.0000	0.1527	0.3407
C0N	0.0005	<.0001	0.0002	0.0342	0.3373	<.0001	<.0001	0.0595	<.0001	0.3468	1.0000	0.8325
C0M	0.0002	<.0001	0.0001	0.0067	0.0138	<.0001	<.0001	0.0050	<.0001	0.0314	<.0001	1.0000

Values are significant at $\alpha < .05$